Fallout tuffs of Trapper Creek, Idaho—A record of Miocene explosive volcanism in the Snake River Plain volcanic province

Michael E. Perkins
William P. Nash
Francis H. Brown
Department of Geology and Geophysics, University of Utah, Salt Lake City, Utah 84112

Robert J. Fleck *U.S. Geological Survey, Menlo Park, California 94025*

ABSTRACT

A 900-m-thick section of tuffaceous sedimentary rock, vitric fallout tuff, and ash-flow tuff is well exposed along Trapper Creek in south-central Idaho. This section provides nearly continuous exposure through the fill of the Goose Creek basin, a major north-trending Miocene extensional basin located along the southern margin of the Snake River Plain volcanic province (SRPVP). Some 51 separate units of vitric fallout tuff are recognized in the Trapper Creek section. Petrographic and chemical characteristics of these vitric tuffs indicate that most are from SRPVP sources. New $^{40}Ar/^{39}Ar$ laser-fusion dating, along with prior isotopic age determinations, show that the Trapper Creek tuffs span the period ca. 13.9–8.6 Ma. Chemical correlation indicates that fallout tuffs in the central part of the Trapper Creek section (12.5–10.0 Ma) are from sources in the Bruneau-Jarbidge volcanic field of the SRPVP centered ≈100 km west of Trapper Creek. Underlying fallout tuffs may have had sources in the Owyhee-Humboldt field of the SRPVP centered ≈200 km west of Trapper Creek, while overlying fallout tuffs, interlayered with several ash-flow tuffs, had a relatively proximal source, possibly in the proposed Twin Falls volcanic field centered ≈60 km north of Trapper Creek.

The Trapper Creek tuffs provide insight into the characteristics of explosive silicic volcanism within the SRPVP during middle–late Miocene time. From ca. 13.9 to ca. 9.5 Ma, major eruptions (those depositing ≥1.5 m of fallout tuff) were frequent (about one event per 200 k.y.); their products display a trend toward the eruption of progressively less evolved, higher temperature silicic magma after 12.5 Ma. This trend to higher temperature eruptions, termed the Cougar Point "flare-up," culminated in the eruption of high-temperature (≈1000 °C), plagioclase-rich magma during the period 10.5–9.5 Ma. In contrast to these eruptions, later (<7.0 Ma) major silicic eruptions within the SRPVP were characterized by the lower temperature (≈850 °C) of the erupted magma and by the longer intervals (about one event per ≈500–600 k.y.) between eruptions. Variations in the character of SRPVP explosive silicic eruptions may reflect changes in the structure, composition, or state of stress in the crust beneath the eastward propagating SRPVP, or, perhaps, changes in the Yellowstone hot-spot plume that may drive the SRPVP volcanism.

INTRODUCTION

Silicic ash-flow tuff and lava and associated capping basalt of Neogene age are abundant and widespread throughout southern Idaho and adjacent parts of Oregon, Nevada, Montana, and Wyoming (Malde and Powers, 1962; Luedke and Smith, 1981, 1982, 1983). Such rocks lie in a broad belt extending from the currently active Yellowstone Plateau volcanic field in Wyoming into southwestern Idaho and adjacent parts of Oregon and Nevada (Fig. 1). This vast volcanic region has been termed the Snake River Plain volcanic province (SRPVP) by Bonnichsen and Kauffman (1987). Geochronologic studies by Armstrong (1975) and Armstrong et al. (1975) first established the eastward age progression of the silicic volcanic rock and associated basalt within this volcanic province. SRPVP silicic volcanism initiated near the common boundary point of Idaho, Nevada, and Oregon at ca. 16 Ma, and progressed east-northeast at an average rate of ≈4 cm/yr, reaching the Yellowstone Plateau area ca. 2 Ma (Rodgers et al., 1990; Pierce and Morgan, 1992; Smith and Braille, 1993). Armstrong et al. (1975) proposed that the rhyolitic volcanic rocks and capping basalt of the SRPVP were generated by a mantle melting spot or mantle plume of the type proposed by Morgan (1972), with the ≈4 cm/yr eastward progression of the volcanism reflecting the motion of the North American plate passing over this thermal anomaly. The thermal anomaly that has generated the silicic volcanic rocks of the SRPVP is now commonly referred to as the Yellowstone hot spot, although not all researchers attribute the Yellowstone hot spot to a deep-seated mantle plume (Hildreth et al., 1991).

Much of the current understanding of SRPVP volcanism is based on studies of the accessible, latest Neogene and Quaternary Yellowstone Plateau volcanic field. Volcanism in this volcanic field, active during the past 2.2 m.y., has been dominated by the eruption of three voluminous, silicic ash-flow tuffs and their associated fallout ash beds (Izett and Wilcox, 1982; Christiansen, 1984). These major pyroclastic eruptions produced three nested calderas, the boundaries of which are still partly exposed and available for direct examination. Other eruptions from the Yellowstone Plateau consisted mainly of quiet outpourings of rhyolite and basalt lava. The style of volcanism associated with the Yellowstone Plateau volcanic field appears to be typical of the next older volcanic field of the SRPVP—the Heise volcanic field located immediately southwest of the Yellowstone Plateau (Fig. 1). Here the eruption of three regionally extensive and several localized silicic ash-flow tuffs occurred between ca. 6.5 and 4.3 Ma (Morgan, 1992). Much of the Heise volcanic field is covered by younger basalt flows and sedimentary fill of the eastern Snake River downwarp, but analysis of geophysical anomalies suggest the existence of

GSA Bulletin; December 1995; v. 107; no. 12; p. 1484–1506; 11 figures; 4 tables.

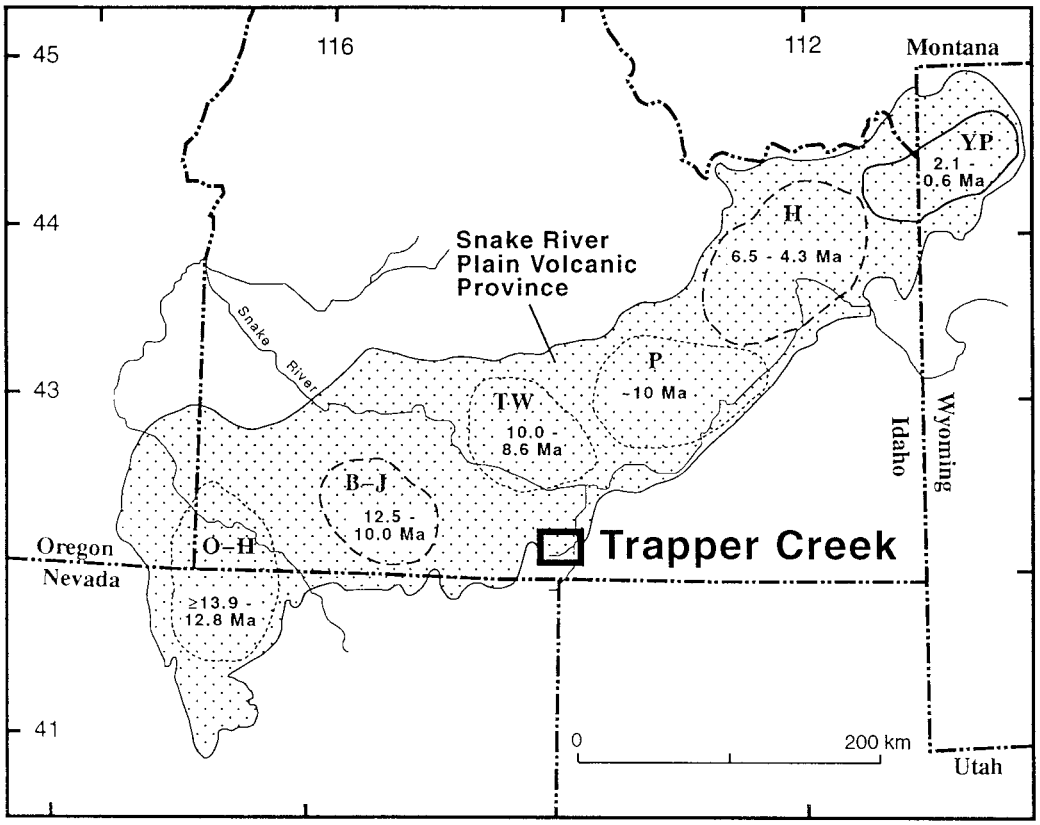

Figure 1. Location Map. Trapper Creek is located at southern edge of the Neogene Snake River Plain silicic volcanic province (stippled area). Proposed major volcanic fields within this province include: Owyhee-Humboldt volcanic field (O-H); Bruneau-Jarbidge volcanic field (B-J); Twin Falls volcanic field (TW); Picabo volcanic field (P); Heise volcanic field (H); and Yellowstone Plateau volcanic field (YP). Degree of confidence in volcanic field boundaries as follows: solid line—best established; long dashed lines—speculative but with some geologic/geophysical evidence presented in support of boundary location; short dashed line—speculative. Adapted from Malde (1986) and Pierce and Morgan (1992). Age range of major explosive activity in the volcanic fields is modified from Pierce and Morgan (1992). Longitude is in degrees west, and latitude is in degrees north.

three large nested calderas at the center of this volcanic field (Morgan et al., 1984).

Older, pre-6.5 Ma volcanic fields of the SRPVP have been proposed (Bonnichsen, 1982a; Bonnichsen and Kauffman, 1987; Ekren et al., 1984; Hackett et al., 1989) and those that have been the source of major explosive eruptions are shown on Figure 1. In addition, Pierce and Morgan (1992) have proposed that peralkaline volcanic fields west of the Owyhee-Humboldt volcanic field and west of the main exposures of the SRPVP may represent the earliest phase of SRPVP volcanism. The ca. 16 Ma McDermitt volcanic field, investigated by Rytuba and McKee (1984) is one such peralkaline volcanic field. Silicic welded ash-flow tuffs comprise a substantial proportion of material erupted from the older SRPVP volcanic fields. Also, a considerable volume of silicic lava appears to have been erupted from both the Bruneau-Jarbidge and Owyhee-Humboldt volcanic fields as well as an intervening area named the Little Jacks eruptive center (Bonnichsen and Kauffman, 1987). Bonnichsen (1982c) and Bonnichsen and Kauffman (1987) have identified numerous large-volume rhyolite lava flows erupted from the Bruneau-Jarbidge volcanic field during a late phase of activity in this field. Further, silicic volcanic rocks of the Owyhee-Humboldt field, originally described as welded tuffs by Ekren et al. (1984), may actually be areally extensive rhyolite flows (Manley, 1992). Available descriptions (Bonnichsen, 1982c; Ekren et al., 1984; Bonnichsen and Kauffman, 1987) indicate these Miocene silicic lavas, like their late Neogene counterparts in the Yellowstone Plateau volcanic field, represent predominantly quiet effusive eruptions with only minor associated pyroclastic debris.

With the exception of the McDermitt volcanic field, well-exposed by block faulting in the extreme western part of the SRPVP, the boundaries of the older volcanic fields, the size and number of associated calderas, and the number, age, and size of associated eruptions are not fully established. As with the Heise field, the proximal silicic units of the older volcanic fields of the SRPVP are extensively obscured by younger basalt flows and sedimentary strata. Hence, the study of such proximal units may not reveal the full extent of silicic volcanism within the Miocene volcanic fields of the SRPVP.

We report here on a sequence of 51 silicic fallout tuffs exposed in the canyon of Trapper Creek in south-central Idaho along the southern margin of the SRPVP (Fig. 1). As discussed below, these fallout tuffs range in age from ca. 13.9 to 8.6 Ma and were mostly generated by explosive eruptions from middle–late Miocene volcanic fields of the SRPVP. Study of the Trapper Creek tuffs provides insight into the early history of SRPVP explosive volcanism, documents changes in magma chemistry and eruption frequency during the evolution of the

TABLE 1. CHEMICAL COMPOSITION OF GLASS FROM SELECTED SAMPLES OF LATE NEOGENE TUFFS

Sample	Electron probe microanalyses*														
	SiO_2 [0.5]	TiO_2 [0.01]	Al_2O_3 [0.2]	Fe_2O_3 [0.03]	MnO [.005]	MgO [0.01]	CaO [0.02]	BaO [0.01]	Na_2O [0.30]	K_2O [0.20]	Cl [.004]	F [0.03]	H_2O [0.7]	–O [0.03]	Total [0.7]
Lava Creek ash bed	73.9	0.12	11.6	1.68	0.04	0.02	0.52	0.01	2.8	5.0	0.13	0.14	4.4	0.09	100.3
Huckleberry Ridge ash bed	73.3	0.11	11.7	1.70	0.04	0.02	0.57	0.02	3.4	4.9	0.14	0.23	3.9	0.13	100.0
Kilgore ash bed	71.3	0.16	11.3	1.40	0.03	0.06	0.51	0.08	3.2	4.9	0.06	0.02	6.8	0.02	99.8
Walcott ash bed	74.1	0.18	11.5	1.21	0.04	0.08	0.48	0.10	3.3	5.1	0.10	0.09	3.0	0.06	99.3
Tuff of Blacktail Creek§	74.5	0.19	11.4	1.27	0.04	0.07	0.46	0.07	3.0	5.5	0.13	N.A.†	3.3	0.03	99.9
Guaje ash bed	73.1	0.07	11.3	1.45	0.07	0.03	0.26	<0.01	3.8	4.5	0.16	0.12	5.3	0.09	100.2
Bishop ash bed	75.2	0.05	12.1	0.74	0.03	0.03	0.42	<0.01	3.1	4.5	0.08	0.04	4.5	0.04	100.8

Sample	X-ray fluorescence spectrometry analyses#														
	Fe [0.03]	Ca [0.02]	Ba [20]	Mn [5]	Nb [1]	Rb [4]	Sr [2]	Ti [30]	Y [5]	Zn [6]	Zr [8]	La [5]	Nd [5]	Th [2]	Ce [15]
Lava Creek ash bed	1.04	0.34	140	250	61	183	6	690	75	70	220	80	65	26	170
Huckleberry Ridge ash bed	1.08	0.36	250	260	54	178	8	780	80	85	225	80	65	25	155
Kilgore ash bed	0.97	0.34	790	245	48	156	21	1000	70	45	275	75	55	23	120
Walcott ash bed	0.71	0.28	840	225	42	167	21	1110	50	45	220	70	55	26	140
Tuff of Blacktail Creek§	0.82	0.30	470	235	37	187	23	1000	60	45	200	60	40	28	140
Guaje ash bed	0.97	0.17	<15	490	94	185	3	480	75	90	250	55	55	23	125
Bishop ash bed	0.45	0.26	<15	255	25	176	2	390	30	35	70	25	20	19	45

Note: Numbers in square brackets are estimated standard deviations of analytical precision, multiple analytical runs (see Appendix B).
*Fe as Fe_2O_3; H_2O estimated by oxygen stoichiometry (Nash, 1992). All concentrations in wt%.
†N.A. = not analyzed.
§Glass of tuff of Blacktail Creek from basal vitrophyre of ashflow tuff; all other glass from fallout tuff.
#Fe and Ca concentrations in wt%, all other concentrations in ppm.

SRPVP, and demonstrates the feasibility of using fallout tuffs as monitors of explosive volcanism in a volcanic province now extensively covered by younger strata.

TERMINOLOGY

The tuffs at Trapper Creek (herein referred to as the Trapper Creek tuffs for convenience) range from middle to late Miocene in age as these time intervals are used by Berggren et al. (1985) and accepted as part of the standard time scale for the Cenozoic for GSA's Decade of North American Geology. As it is awkward to repeatedly refer to the Trapper Creek tuffs as being middle–late Miocene in age or to repeatedly refer to the middle–upper Miocene Trapper Creek tuffs, we use Miocene when referring, in general, to the age of the Trapper Creek tuffs or the stratigraphic position of the Trapper Creek tuffs within the Miocene. When it is necessary to refer to specific intervals of the Miocene then the appropriate adjectives of early/lower, middle/middle, or late/upper are used.

ANALYTICAL METHODS

Sample Preparation

A glass fraction of ≥99.5% purity was prepared by crushing each sample in a mullite mortar and sieving through 18, 35, 60, 120, and 230 (or 170) size brass sieves. The 60–120 fraction (rarely the 120–230 fraction) was treated in 10% (V/V) HNO_3 for 15–20 min and washed thoroughly in distilled water to remove any carbonate minerals. Then the samples were treated with 5% (V/V) HF in an ultrasonic cleaner to remove surficial clay alteration, washed repeatedly in distilled water, and dried at 80 °C. Repeated passes through a Frantz Isodynamic Separator™ removed magnetic and nonmagnetic minerals from the glass. Purity of each sample was checked with a petrographic microscope. When present, glass shards with feldspar inclusions were finally removed using organic heavy liquids.

A few milligrams of the glass separate were mounted with epoxy on a plastic disk and polished for electron probe microanalysis. Another 2.0–2.4 g of glass was mixed with cellulose in a 4:1 ratio, ground in a mullite mortar, and pressed into a 3.2-cm-diameter pellet for X-ray fluorescence analysis. Sanidine crystals 0.5–1.0 mm in size were concentrated with heavy liquid, and clear crystals with <1% included glass were hand picked from this concentrate for dating. These crystals were treated in 10% (V/V) HF for 10 min in an ultrasonic cleaner to remove adhering glass and then cleaned in deionized water for 30 min.

Instrumental Techniques

For electron probe microanalysis, a Cameca SX-50 (University of Utah) was used to measure Si, Ti, Al, Fe, Mn, Mg, Ca, Ba, Na, K, Cl, F, and O. Typically, 20 shards were analyzed from each sample. Nash (1992) describes the analytical conditions used. Estimates of H_2O content of these hydrated glass shards were calculated from the difference between measured and stoichiometric oxygen contents. An ARL 8410 XRF spectrometer was used to measure Fe, Ca, K, Ba, Mn, Nb, Rb, Sr, Ti, Zn, Zr, La, Nd, Th, and Ce. A suite of standards, analyzed by instrumental neutron activation (La, Ce, Nd, Th), standard addition (Nb, Rb, Sr, Y, Zr, Ba), X-ray fluorescence spectrometry (Ti, Zn), or wet chemistry (Fe, Ca, K, Mn), were used as primary reference standards. Glass from seven U.S. tuffs were calibrated to the primary standards. These secondary standards were used to calibrate the X-ray fluorescence analyses of the Trapper Creek tuffs. Table 1 shows our analyses of glass from several easily obtainable and well-characterized late Neogene ash beds. Other workers can use these analysis to facilitate interlaboratory comparisons of electron probe microanalysis and X-ray fluorescence results.

$^{40}Ar/^{39}Ar$ ages were determined on small groups of sanidine grains in the laser-fusion $^{40}Ar/^{39}Ar$ system at the U. S. Geological Survey, Menlo Park, California. The methods and equipment used were essentially the same as described by Dalrymple and Duffield (1988). Error estimates for each age include an uncertainty of 0.5% on the value of J, the irradiation constant. Samples were irradiated for 16 hr at the U.S. Geological Survey TRIGA reactor in Denver, Colorado. Ar isotopes were corrected for neu-

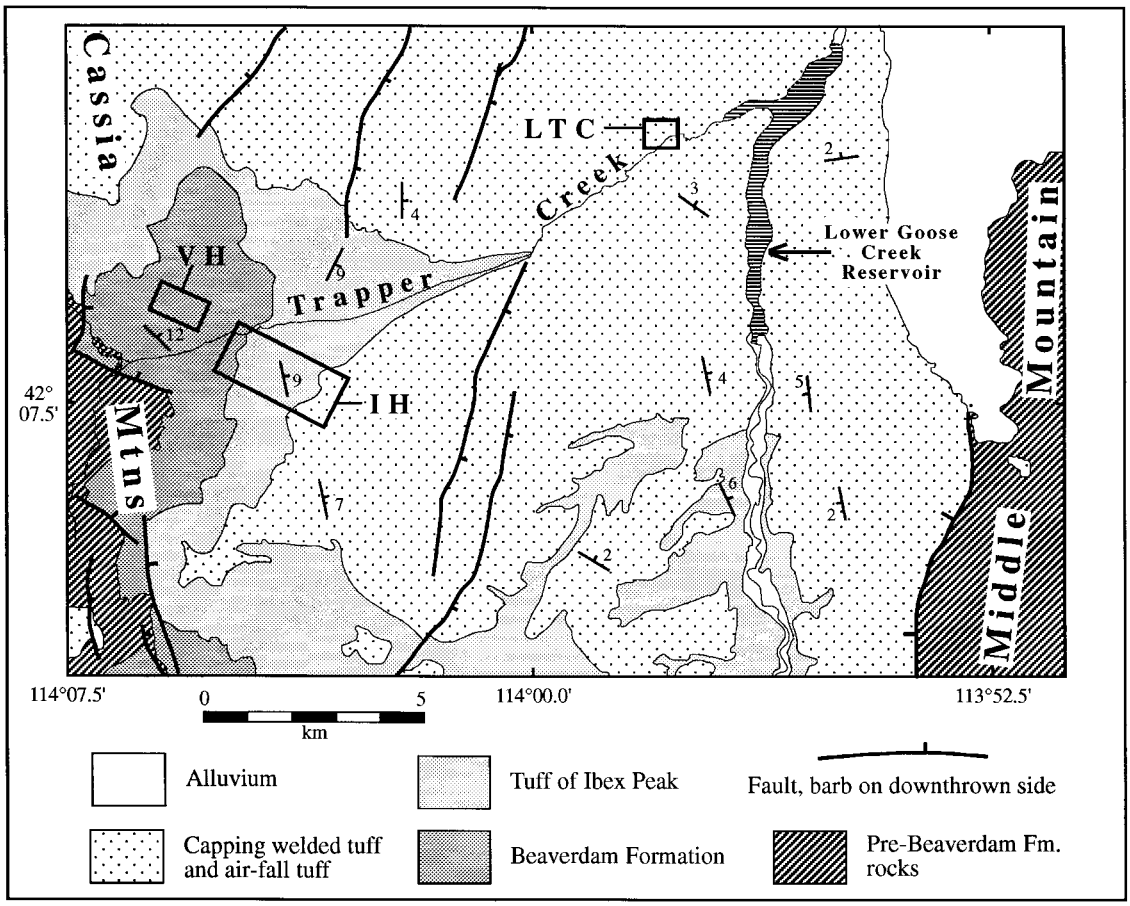

Figure 2. Generalized geologic map of Trapper Creek area. Areas of measured sections are indicated by boxes: VH, Violets Hollow and vicinity; IH, Ibex Hollow and vicinity; LTC, Lower Trapper Creek. Adapted from Mapel and Hail (1959), Williams et al. (1990), and Saltzer and Hodges (1988). Pre-Beaverdam Formation rocks include rhyolite correlated with the middle Miocene Jarbidge Rhyolite by Axelrod (1964). Longitude in degrees west, and latitude in degrees north.

tron reactions with Ca and K using correction factors measured on K-glass and CaF_2 irradiated along with the samples. ^{37}Ar was corrected for decay during and after irradiation. Neutron flux was calculated from analyses of the Menlo Park standard sanidine monitor, 85G003 (Taylor Creek Rhyolite; 27.92 Ma), placed throughout the stack of samples in the quartz-glass irradiation vial. Calibrations of this standard are tied to those of the usual conventional K-Ar standards used in this laboratory (Lanphere et al., 1990). Using these calibrations, the age calculated for Minnesota standard hornblende, MMhb-1, is 513.9 Ma, whereas Sampson and Alexander (1987) cite an average of 520.4 ± 1.7 Ma. Isotopic decay and abundance constants recommended by Steiger and Jager (1977) were used.

GEOLOGIC SETTING

Trapper Creek flows eastward in a high-walled canyon incised into the east flank of the Cassia Mountains and joins Goose Creek, a northward-flowing tributary of the Snake River (Fig. 2). Excellent exposures of the tuffaceous sedimentary rocks, fallout tuff, and ash-flow tuff of the Miocene Goose Creek basin occur locally in the canyon of Trapper Creek. To the west, the Goose Creek basin onlaps onto Lower Permian unmetamorphosed sedimentary rocks at the center of the 2400-m-high Cassia Mountains (Fig. 2; Mytton, et al., 1990; Williams et al., 1990). To the east, the Goose Creek basin onlaps onto older rocks exposed in the 2400-m-high Middle Mountain. These older rocks consist of intensely deformed Paleozoic strata and Tertiary granitic intrusions that comprise part of the middle Tertiary Albion Range–Raft River Range metamorphic core complex (Saltzer and Hodges, 1988). Rhyolite, correlated with the middle Miocene Jarbidge Rhyolite by Axelrod (1964), unconformably overlies the core complex rocks of Middle Mountain and unconformably underlies the sedimentary rocks of the Goose Creek basin. The 400- to 900-m-thick fill of the basin generally dips gently eastward off the flank of the Cassia Mountains into a zone of north-trending faults along the western flank of Middle Mountain and the Goose Creek Mountains to the south (Fig. 2; Mapel and Hail, 1959). A buttress unconformity and some faulting mark the western margin of the basin (Mapel and Hail, 1959; Mytton et al., 1990).

Terminology of the Goose Creek basin deposits has changed with each new investigation (see review in Hildebrand and Newman, 1985), but all workers since Mapel and Hail (1959) have recognized the basic threefold division of these deposits (Figs. 2 and 3). The oldest unit, named the Beaverdam Formation of Axelrod (1964) by Mytton et al. (1990), consists of tuffaceous shale and sandstone with some lignite, carbonaceous shale, conglomerate, and ash-sized (<2 mm) gray vitric fallout tuff. Outcrops of the Bea-

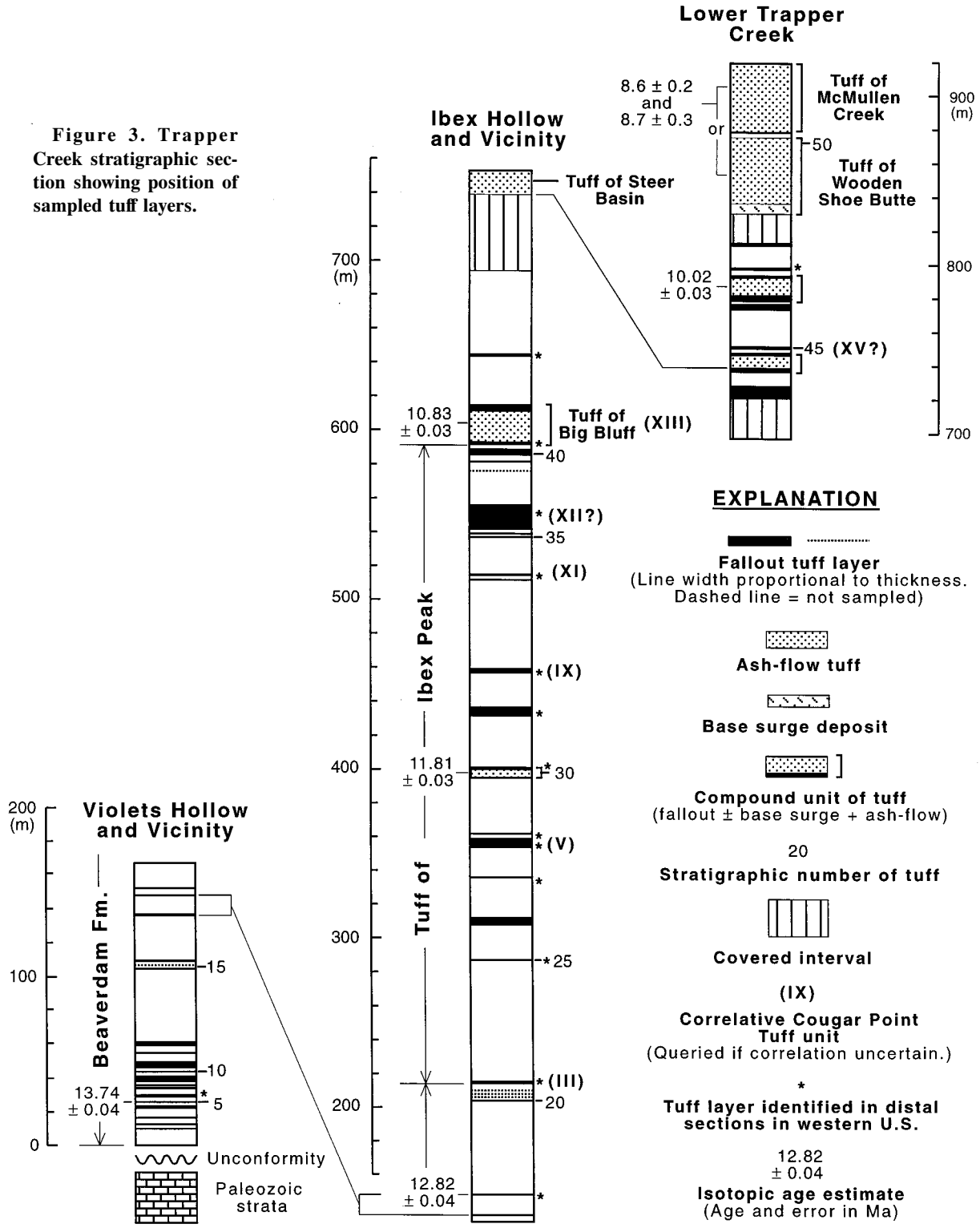

Figure 3. Trapper Creek stratigraphic section showing position of sampled tuff layers.

verdam Formation are restricted to the west side of the basin. The middle unit, named the tuff of Ibex Peak by Mytton et al. (1990) and Williams et al. (1990), consists of ash-sized, gray, vitric tuff and its reworked equivalent along with lesser amounts of tuffaceous shale, lignite, conglomerate, and unwelded ash-flow tuff. The tuff of Ibex Peak occurs throughout the Goose Creek basin. The upper unit consists of a sequence of welded ash-flow tuff, ash-sized, gray vitric fallout tuff, reworked tuff, and minor conglomerate and tuffaceous shale. Four areally extensive ash-flow tuffs in the upper unit have been named by Mytton et al. (1990) and Williams et al. (1990). From base to top, these are the tuff of Big Bluff, the tuff of Steer Basin, the tuff of Wooden Shoe Butte,

and the tuff of McMullen Creek (Fig. 3). This upper sequence extends beyond the margins of the Goose Creek basin to both the east and west.

Sedimentological analysis of the Goose Creek basin by Hildebrand and Newman (1985) indicate interfingering fluvial and lacustrine environments existed within the basin. Several workers (Axelrod, 1964; Hildebrand and Newman, 1985; Rodgers et al., 1991) have proposed that drainage was generally southerly during basin filling. Hildebrand and Newman (1985) interpret the Goose Creek basin to be a fault-bounded basin that formed in response to Miocene extension. Rodgers et al. (1990) concur with this interpretation and propose that it formed in response to crustal stresses generated in front of the east-northeast–propagating Yellowstone hot spot.

THE TRAPPER CREEK TUFFS

Measured Sections

The tuffs in the Trapper Creek area were studied in three sections (Figs. 2 and 3) originally measured by Mapel and Hail (1959). These sections, which afford a nearly complete exposure of strata of the Goose Creek basin in the Trapper Creek area, were remeasured for this study. Fifty-one fallout tuffs were identified in the 900-m-thick composite Trapper Creek section (Fig. 3), and all of the thicker tuffs (those generally with fallout layers >30 cm thick) were collected for petrographic and chemical analyses. For reference, each identified tuff horizon is given a stratigraphic number starting with 1 at the base and ranging in sequence to 51 at the top. Most tuffs consist of a basal fallout unit, an overlying reworked zone, and in some cases a capping argillic paleosol. For these tuffs only the basal fallout layer is shown on the composite section (Fig. 3). Six of the numbered tuff horizons include an ash-flow tuff unit. The upper five of these ash-flow tuffs are welded tuffs. All of the ash-flow tuffs have an associated underlying (basal) fallout tuff, and several have an overlying (co-ignimbrite?) fallout tuff that may be capped by reworked tuff and an argillic paleosol. For these compound tuff horizons the fallout and ash-flow tuff units are shown on the composite section. Finally, one tuff horizon, tuff 50 (tuff of Wooden Shoe Butte), includes a base-surge deposit between the basal fallout tuff and the overlying ash-flow tuff.

The general location of the three sections comprising the composite Trapper Creek section is shown on Figure 2, and additional information on their locations is given in Appendix A. The basal 170 m of the Trapper Creek section, all within the Beaverdam Formation, is exposed in Violets Hollow and vicinity. The basal section is faulted, but detailed mapping and chemical correlation of tuffs across faults has permitted a reconstruction of the stratigraphic sequence. The middle 600 m of the section is exposed in Ibex Hollow and vicinity, 2 km west of Violets Hollow. In this section the uppermost 50 m of the Beaverdam Formation, the entire tuff of Ibex Peak, and the basal 150 m of the capping sequence of interlayered ash-flow tuffs and fallout tuffs are nearly continuously exposed, with only one easily identifiable fault duplicating a small part of the section. The uppermost 200 m of the section is exposed in the lower part of Trapper Creek canyon ≈2 km west of the confluence of Trapper Creek and Goose Creek.

Two fallout ashes, tuff 17 and tuff 18, tie the Violets Hollow section to the Ibex Hollow section (Fig. 3). Correlation between the Ibex Hollow section and the Lower Trapper Creek section is somewhat more problematic. X-ray fluorescence analyses (see Table 3 below) indicate that vitrophyre glass from the tuff of Steer Basin at the top of the Ibex Hollow section (sample TC89-36) best matches vitrophyre glass from a previously unrecognized ash-flow tuff near the base of the Lower Trapper Creek section (sample TC90-15). However, the chemical match is not exact, and it is possible that either the tuff of Steer Basin is not present in the upper section or that the next higher welded tuff (sample TC90-20) is the tuff of Steer Basin—this latter correlation was made by Mapel and Hail (1959). A more definitive correlation between the upper two sections awaits discovery of an outcrop of basal fallout tuff unit of the tuff of Steer Basin in the Ibex Hollow area. We have found that fallout tuffs have a more consistent glass composition than the often incipiently devitrified vitrophyres of ash-flow tuffs and, hence, are more useful for correlation of welded ash-flow tuffs.

AGE OF THE TRAPPER CREEK SECTION

Previous Age Estimates

Prior to this study the age range of the Goose Creek basin strata was not well established. Fossils reported from a few localities by Mapel and Hail (1959), Axelrod (1964), Campbell (1979), and Hildebrand and Newman (1985) generally indicate a Miocene age for the tuffaceous sedimentary rocks underlying the capping welded tuffs of the Goose Creek basin. K-Ar dates ranging from 10.1 to 8.6 Ma (new constants) are reported for the uppermost welded ash-flow tuffs of the Trapper Creek section (Armstrong, 1975; Armstrong et al., 1975, 1980), while G. B. Dalrymple reports (in Williams et al., 1990) dates of 12.0 ± 0.4 Ma and 16.2 ± 0.5 Ma, respectively, for the underlying tuff of Steer Basin and tuff of Big Bluff.

The description of localities given by Armstrong (1975) and Armstrong et al. (1975, 1980) is not always sufficient to establish which ash-flow tuffs were dated. Samples yielding the two youngest age dates, 8.4 ± 0.2 Ma (8.6 Ma, new constants) and 8.5 ± 0.3 Ma (8.7 Ma, new constants), are probably from the uppermost two ash-flow units, but which unit (or units) was dated is not clear. Mytton et al. (1990) assign both K-Ar dates to the tuff of McMullen Creek, while Hildebrand and Newman (1985) assign both to the underlying tuff of Wooden Shoe Butte. We suspect both dates should be assigned to the tuff of McMullen Creek, but either option may be correct, as indicated on Figure 3. The older K-Ar date of 10.1 ± 0.2 Ma reported by Armstrong et al. (1980) is most likely from an unnamed ash-flow tuff along Trapper Creek road (tuff 47 on Fig. 3). Mytton et al. (1990) suggest that the overlying tuff of Wooden Shoe Butte was the tuff dated at 10.1 Ma, but this seems unlikely. Armstrong et al. (1980) report the sample was collected along Trapper Creek road, and tuff 47 is the only prominently welded tuff cropping out near road level in the area from which the sample was collected. Results of $^{40}Ar/^{39}Ar$ laser-fusion age dating of tuff 47, presented below, support the conclusion that tuff 47 was indeed the tuff dated by Armstrong et al. (1980) at 10.1 Ma.

Dalrymple (*in* Williams et al., 1990) reports a K-Ar date of 12.0 ± 0.4 Ma on the tuff of Steer Basin and one of 16.2 ± 0.5 Ma on the tuff of Big Bluff. These are the lowest two welded ash-flow tuffs in the Trapper Creek section (Fig. 3). No information is given on the location of the dated samples or on the material used for the age dating. These results, particularly the 16.2 Ma date for the tuff of Big Bluff, indicate an early Miocene or older age for the lower part of the Trapper Creek section. This is in conflict

TABLE 2. RESULTS OF $^{40}Ar/^{39}Ar$ LASER-FUSION ANALYSES

Run numbers	Grains	$^{40}Ar^*$ (mol)	K/Ca	$^{40}Ar^*$ (%)	$^{40}Ar/^{39}Ar$	$^{37}Ar/^{39}Ar$	$^{36}Ar/^{39}Ar$	Age† (Ma)
TC90-20/92, stratigraphic number 47; J = 0.003416								
73A	3–4	9.485E-14	14.10	95.9	1.70284	0.03475	2.265E-04	10.04 ± 0.07
73B	2	1.053E-13	14.98	95.5	1.70555	0.03272	2.513E-04	10.01 ± 0.06
73C	2–3	7.289E-14	15.27	94.9	1.72076	0.03209	2.910E-04	10.03 ± 0.07
73D	2	9.986E-14	15.32	99.6	1.64490	0.03198	1.214E-05	10.09 ± 0.06
73E	1	1.443E-13	14.41	99.1	1.64455	0.03400	4.111E-05	10.02 ± 0.06
73F	2	9.911E-14	14.34	94.4	1.71640	0.03416	3.180E-04	9.96 ± 0.07
							Wtd.mean	10.02 ± 0.03
							MSWD§	0.43
TC89-32/92, stratigraphic number 41; J = 0.003421								
72A	2	2.431E-13	8.11	35.4	4.92806	0.06041	1.078E-02	10.72 ± 0.12
72B	2	1.047E-13	14.19	74.1	2.36039	0.03452	2.064E-03	10.76 ± 0.07
72C	3	8.321E-14	12.80	97.9	1.79934	0.03829	1.188E-04	10.84 ± 0.07
72D	2–3	6.429E-14	14.49	51.4	3.46648	0.03382	5.690E-03	10.97 ± 0.10
72E	2	1.013E-13	13.00	98.1	1.78751	0.03770	1.062E-04	10.79 ± 0.07
72F	3	9.264E-14	14.01	97.7	1.81295	0.03498	1.363E-04	10.89 ± 0.07
							Wtd.mean	10.83 ± 0.03
							MSWD	0.99
TC89-21B, stratigraphic number 30; J = 0.003432								
71A	5–6	1.360E-13	13.92	98.9	1.93986	0.03521	6.776E-05	11.83 ± 0.07
71B	6	1.319E-13	5.53	98.1	1.95796	0.08863	1.319E-04	11.85 ± 0.07
71C	4–5	1.756E-13	13.58	98.7	1.93867	0.03608	7.552E-05	11.81 ± 0.07
71D	4–5	1.553E-13	12.84	98.9	1.93717	0.03815	6.688E-05	11.82 ± 0.07
71E	4–5	1.266E-13	12.26	98.9	1.92895	0.03997	6.821E-05	11.77 ± 0.07
71F	3–4	9.663E-14	2.96	99.0	1.93171	0.16556	9.457E-05	11.80 ± 0.08
							Wtd.mean	11.81 ± 0.03
							MSWD	0.16
TC89-20A, stratigraphic number 18; J = 0.003437								
44B	5	6.057E-14	17.85	98.9	2.08797	0.02746	6.725E-05	12.76 ± 0.10
44C	4–5	7.290E-14	17.73	98.8	2.10724	0.02764	7.743E-05	12.86 ± 0.09
44D	4–6	5.218E-14	19.06	99.7	2.09255	0.02571	9.859E-06	12.89 ± 0.10
44E	5–6	8.400E-14	18.79	99.7	2.07973	0.02608	1.382E-05	12.80 ± 0.09
44F	4–5	5.104E-14	18.42	98.1	2.11004	0.02659	1.263E-04	12.79 ± 0.10
							Wtd.mean	12.82 ± 0.04
							MSWD	0.30
TC90-40, stratigraphic number 5; J = 0.003410								
74A	3	8.937E-14	18.30	98.6	2.29031	0.02677	1.019E-04	13.83 ± 0.09
74B	3–4	1.492E-13	21.81	98.7	2.27698	0.02247	9.100E-05	13.77 ± 0.08
74C	3–4	1.260E-13	19.17	98.5	2.27464	0.02556	1.076E-04	13.73 ± 0.09
74D	4	1.275E-13	21.67	98.1	2.29045	0.02261	1.388E-04	13.77 ± 0.09
74E	4	9.116E-14	18.33	97.5	2.27609	0.02673	1.843E-04	13.60 ± 0.09
74F	4–5	1.184E-13	19.96	98.3	2.27804	0.02455	1.200E-04	13.73 ± 0.09
							Wtd.mean	13.74 ± 0.04
							MSWD	0.76

*Radiogenic ^{40}Ar.

†Correction factors for neutron produced isotopes: $(^{39}Ar/^{37}Ar)\ Ca = 0.00067$, $(^{36}Ar/^{37}Ar)\ Ca = 0.000269$, $(^{40}Ar/^{39}Ar)\ K = 0.0051$.

§MSWD is mean square of the weighted deviates of individual runs.

with paleontologic evidence that strata beneath the capping welded tuffs are best regarded as middle–late Miocene in age. Results of $^{40}Ar/^{39}Ar$ dating presented below indicate that the K-Ar ages reported for the tuff of Steer Basin and the tuff of Big Bluff are too old.

$^{40}Ar/^{39}Ar$ Laser-Fusion Ages

Sanidine was separated from five tuffs in the Trapper Creek section for $^{40}Ar/^{39}Ar$ laser-fusion dating. Tuffs were selected that contained sanidine coarse enough (≥0.5 mm) to be suitable for the laser-fusion technique. The tuffs dated include two fallout tuffs from the Beaverdam Formation (tuffs 6 and 19), a nonwelded ash-flow tuff in the middle part of the tuff of Ibex Peak (tuff 30), the tuff of Big Bluff (tuff 41), and the welded ash-flow tuff along Trapper Creek road (tuff 47) that we believe was the same tuff previously dated at 10.1 ± 0.2 Ma by Armstrong et al. (1980). The locations of the dated samples are given in Appendix A, and their stratigraphic positions are shown in Figure 3. Tuffs above the highest dated tuff lack sanidine, and the relatively low K content (≈1%) of the abundant plagioclase in these tuffs makes them unsuitable for laser-fusion dating. Additional studies using resistance-furnace heating could provide high-precision age control for the youngest tuffs in the section.

Measured $^{40}Ar/^{39}Ar$ ages range from 13.74 ± 0.04 Ma for the stratigraphically lowest dated sample to 10.02 ± 0.03 Ma for the stratigraphically highest dated sample (Table 2). The results appear analytically sound, and ages give a reasonable depth versus age relationship (Fig. 4). Further, these age dates are in general agreement with the fossil evidence and within the range predicted previously for these tuffs on the basis of chemical correlation with tuffs in other sections in the Basin and Range Province that have paleontologic and/or isotopic age control (Perkins et al., 1993). The $^{40}Ar/^{39}Ar$ age date of 10.02 ± 0.03 Ma for sample TC90-20/92 agrees with the K-Ar date of 10.1 ± 0.1 Ma determined by Armstrong et al. (1980) and supports our contention that their K-Ar date was on the unnamed welded tuff outcropping along Trapper Creek Road and not the overlying tuff of Wooden Shoe Butte as assumed by Williams et al. (1990). On the basis of these observations we conclude that the $^{40}Ar/^{39}Ar$ age dates provide reasonable, high-precision dates for the Trapper Creek section. The dates reported for the tuff of Big Bluff (16.2 ± 0.5 Ma) and the tuff of Steer Basin (12.0 ± 0.4 Ma) by Williams et al. (1990) do not provide reasonable age estimates for these tuffs.

DESCRIPTION OF TUFFS

Fifty-one distinct tuffs have been identified in the Goose Creek basin deposits exposed in Trapper Creek—23 in the Beaverdam Formation, 17 in the tuff of Ibex Peak, and 11 in the capping ash-flow/fallout tuff sequence (Fig. 3). These tuffs, as discussed above, are compound horizons that variously include primary pyroclastic debris, such as fallout and ash-flow tuff, and secondary pyroclastic debris in the form of reworked tuff and tuffaceous paleosols. The fallout tuffs are friable to weakly consolidated, ash-sized, vitric tuffs that generally contain <10% crystals, mostly feldspar and quartz. They are generally gray, although particularly fine-grained tuffs and tuffs that contain substantial clay matrix appear white. The Trapper Creek fallout tuffs are generally 0.5–5 m thick and have a median size in the fine sand to very fine sand range (0.25–0.125 mm). There is no obvious relationship between thickness, grain size, or crystal content as a function of stratigraphic position in the fallout tuffs of Trapper Creek. Alternating thin layers or laminae of coarser and finer ash with either parallel layering or very low-angle cross layering are common in the

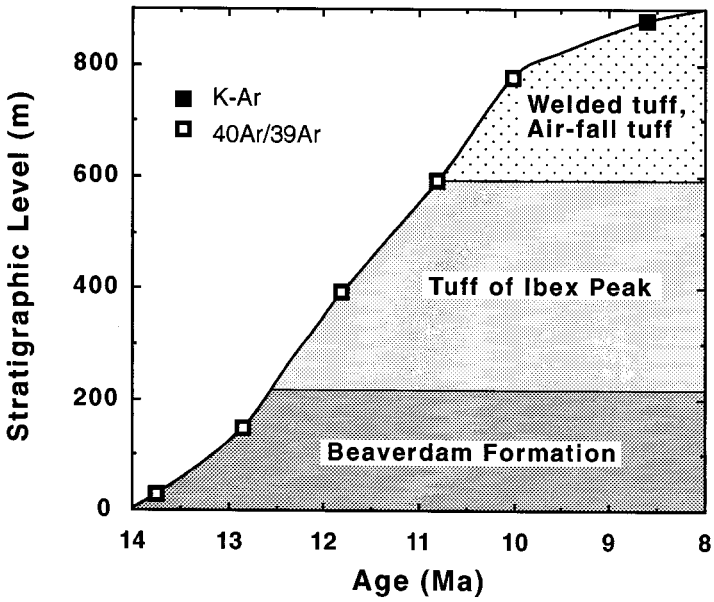

Figure 4. Age versus height in Trapper Creek section.

fallout tuffs. As finer ash is distinctly lighter in color than coarser ash, the bedded fallout tuffs have a distinctive light-dark banding. A layer of reworked vitric tuff commonly overlies the fallout tuff. This reworked tuff may be either massive (bioturbated?), faintly bedded, or cross-bedded. Faint to well-defined burrow(?) fillings are not uncommon in massive reworked tuff. Bedded reworked tuff generally lacks the distinctive alternating darker (coarser) and lighter (finer) layers of fallout tuff, and hence is a more uniform gray than the fallout tuff. A sharp, undulatory surface often marks the contact between primary fallout and reworked bedded tuff. The reworked tuffs are generally thicker than the underlying fallout tuff, attaining thicknesses up to 40 m. Fallout tuff units are often capped by a pale brown to brown argillic paleosol. Massive bioturbated tuff beneath such paleosols is distinctly browner and richer in clay than underlying fallout tuff.

Five welded ash-flow tuffs are present in the upper part of the section above the tuff of Ibex Peak, and an unwelded ash-flow tuff is present in the middle part of the tuff of Ibex Peak. These ash-flow tuffs are a few meters to 40 m thick. The welded tuffs consist primarily of dull, gray to reddish brown, devitrified welded tuff with thin basal and capping units of dark gray to black vitrophyre. Where <5 m thick, however, they consist primarily of vitrophyre. Phenocrysts in the ash-flow tuffs consist of $\leq 10\%$ feldspar and quartz with minor amounts of augite, opaque iron oxides, and zircon. Exposures of the basal contact of the welded tuffs show welded tuff resting directly on fallout tuff, the upper 10–30 cm of which is consistently welded to a dark grayish brown vitrophyre in which the relict parallel layering of the fallout tuff is readily visible. The change in color from gray to dark grayish brown likely results from the formation of nanometer-sized magnetite in the glass as a consequence of heating to high temperature in the presence of oxygen (Schlinger et al., 1988). The unwelded ash-flow tuff in the middle part of the tuff of Ibex Peak is a massive, dark brown, 4-m-thick tuff that caps a 20-m-thick, 500-m-wide channel fill complex exposed in the Ibex Hollow area.

Petrology

During sample preparation the tuffs were split into three fractions (magnetic, glass, and nonmagnetic) using a Frantz Isodynamic Separator. The magnetic fraction of the fallout tuffs typically represents a trace to 2% of the sample, and generally consists of (1) dark gray to brown, flow-banded obsidian fragments; (2) brown to dark brown bubble wall, platy, or bubble junction glass shards; (3) nearly colorless glass shards containing minute Fe-Ti oxide inclusions; (4) magnetite and/or ilmenite with or without a glass jacket; and (5) quartz and feldspar with inclusions of Fe-Ti oxides. Mafic silicate minerals are rare and consist of a trace amount of either clinopyroxene or hypersthene.

The nonmagnetic fraction of the fallout tuffs represents typically a trace to 10% of the sample and consists primarily of feldspar and quartz. Zircon is observed commonly as a trace component in this fraction, and a small percentage of felsic volcanic and/or argillaceous rock fragments is common. Both sanidine and plagioclase cleavage fragments are noted. Quartz is present often as complete or broken dipyramids, but fragments without crystal faces are sometimes present. Melt inclusions of brown glass are sometimes present in quartz and feldspar and in some samples are particularly abundant in plagioclase. In the ash-flow tuffs plagioclase typically displays a "sieve" texture, with a network of brown glass thoroughly interspersed through the mineral. Microprobe analyses of feldspar from several fallout tuffs show that the alkali feldspar is mildly sodic sanidine, and the plagioclase is calcic oligoclase to sodic andesine.

Glass shards in the fine sand-sized fraction are predominantly what we term *ridged* or *striated* shards with lesser amounts of pumice and bubble wall shards. The striated shards are fragments of pumiceous glass that had vesicles consisting of highly elongated, parallel tubules. Such pumice shatters into elongate shards during eruption, breaking along the long axes of the vesicles. Surfaces of these shards have a pronounced cylindrical grooving, the interior of the elongated vesicles forming the grooves. The septa of glass between the vesicles form long, thin, parallel ridges on the surface of the shards, giving them a striated appearance when examined under immersion oil. The color of the bulk glass, after removal of adhering clay, varies from light gray to gray (N7/0 to N5/0 Munsell color) with light gray being observed only in glass with low iron concentration (Fe < 1.0 wt%). The luster is generally dull except for the few tuffs dominated by bubble wall glass shards. A pronounced micaceous luster is characteristic of these latter tuffs because of the efficient reflection of light off the flat or slightly curved plates.

Composition of Glass

Representative electron probe microanalyses and X-ray fluorescence analyses of glass shards from the Trapper Creek tuffs are given in Table 3. Electron probe microanalyses of major and minor element concentrations of the Trapper Creek glass shards show them to consist of hydrated, high-silica, metaluminous to subaluminous rhyolitic

TABLE 3. CHEMICAL COMPOSITION OF GLASS FROM SELECTED SAMPLES OF THE TRAPPER CREEK TUFFS

Sample	SNO*	Type†	Electron probe microanalyses														
			SiO_2 [0.5]	TiO_2 [0.01]	Al_2O_3 [0.2]	Fe_2O_3 [0.03]	MnO [.005]	MgO [0.01]	CaO [0.02]	BaO [0.01]	Na_2O [0.30]	K_2O [0.20]	Cl [.004]	F [0.03]	H_2O [0.7]	–O [0.03]	Total [0.7]
TC92-71	51	v	72.3	0.30	11.6	2.53	0.03	0.11	0.88	0.08	2.8	5.4	0.04	0.09	3.0	0.05	99.2
TC90-20	47§	af	72.5	0.30	11.6	2.26	0.03	0.10	0.78	0.08	2.6	6.0	0.03	0.06	2.6	0.03	99.0
TC90-17	45	f	72.2	0.29	11.5	2.21	0.03	0.12	0.73	0.07	2.4	5.5	0.02	0.11	6.5	0.05	101.6
TC92-15c	44	v	72.2	0.32	11.5	2.39	0.03	0.10	0.83	0.08	2.6	5.9	0.02	0.11	3.0	0.05	99.0
TC89-36a	44	v	73.5	0.34	11.8	1.02	0.02	0.01	0.30	0.06	2.6	6.3	0.03	0.11	3.3	0.05	99.4
TC89-34a#	42	f	72.4	0.31	11.4	2.48	0.04	0.09	0.80	0.06	2.2	5.5	0.02	0.18	5.0	0.08	100.4
TC89-33b	41§	c	72.9	0.19	11.4	2.06	0.03	0.03	0.62	0.02	2.4	5.5	0.04	0.20	5.0	0.09	100.3
TC89-31a#	41§	f	72.9	0.19	11.5	2.08	0.03	0.03	0.63	0.02	2.4	5.6	0.04	0.22	4.8	0.10	100.3
TC89-28a#	37	f	71.5	0.30	11.4	2.11	0.04	0.11	0.73	0.07	2.5	5.6	0.02	0.12	6.2	0.06	100.6
TC89-27c#	34	f	73.0	0.20	11.4	1.92	0.03	0.05	0.58	0.02	2.2	5.9	0.04	0.21	5.0	0.10	100.4
TC89-25a#	32	f	73.0	0.23	11.4	1.82	0.03	0.07	0.55	0.02	2.1	6.1	0.03	0.20	5.0	0.09	100.4
TC89-24a#	31	f	71.6	0.32	11.4	2.03	0.03	0.11	0.70	0.05	2.3	5.9	0.02	0.12	6.1	0.06	100.5
TC89-21b	30§	af	72.6	0.26	11.4	2.12	0.04	0.07	0.70	0.07	2.2	6.5	0.03	0.05	3.4	0.03	99.5
TC89-21a#	30§	f	71.4	0.24	11.2	2.04	0.04	0.06	0.60	0.04	2.2	6.1	0.03	0.13	7.1	0.06	101.1
TC89-19b#	29	f	72.9	0.24	11.4	1.56	0.02	0.09	0.52	0.03	1.8	6.5	0.03	0.12	5.6	0.06	100.8
TC89-18a#	28	f	73.3	0.20	11.5	1.88	0.03	0.06	0.59	0.07	2.3	6.2	0.05	0.28	5.3	0.13	101.5
TC89-17a#	27	f	72.3	0.27	11.7	1.77	0.03	0.12	0.66	0.04	1.9	6.4	0.04	0.17	5.7	0.08	101.0
TC89-16a	26	f	73.0	0.22	11.4	1.56	0.02	0.08	0.52	0.02	1.7	6.6	0.03	0.17	5.6	0.08	100.8
TC89-15#	25	f	72.8	0.22	11.4	1.62	0.02	0.08	0.55	<0.01	1.4	6.7	0.04	0.24	5.4	0.11	100.4
TC89-12#	24	f	71.2	0.17	11.4	1.44	0.03	0.06	0.50	0.01	1.8	6.8	0.06	0.20	6.5	0.10	100.1
TC89-20a#	18§	f	72.2	0.17	11.3	1.68	0.03	0.04	0.53	0.01	1.6	7.0	0.06	0.18	5.0	0.09	99.8
TC90-40	5§	f	72.0	0.10	11.3	1.62	0.02	0.02	0.55	0.01	1.5	7.2	0.10	0.25	5.5	0.13	100.1
TC92-135	1	f	71.3	0.23	11.0	2.18	0.03	0.05	0.63	0.10	1.4	6.9	0.03	0.20	7.0	0.09	100.9

Sample	SNO*	Type†	X-ray fluorescence spectrometry analyses														
			Fe [0.03]	Ca [0.02]	Ba [20]	Mn [5]	Nb [1]	Rb [4]	Sr [2]	Ti [30]	Y [5]	Zn [6]	Zr [8]	La [5]	Nd [5]	Th [2]	Ce [15]
TC92-71	51	v	1.69	0.65	1050	320	44	151	55	1780	55	50	510	70	65	26	165
TC90-20	47§	af	1.74	0.67	1110	310	41	162	56	1890	55	50	545	70	65	28	150
TC90-17	45	f	2.05	0.73	1070	220	42	173	50	1730	60	50	475	75	55	26	140
TC92-15c	44	v	1.90	0.64	1060	180	39	175	46	1700	55	35	430	70	55	27	140
TC89-36a	44	v	1.92	0.62	1080	155	40	175	47	1740	55	40	455	70	50	26	135
TC89-34a#	42	f	1.54	0.54	1130	210	36	168	44	1680	50	45	465	90	50	28	140
TC89-33b	41§	c	1.29	0.41	600	190	38	181	23	1120	65	65	370	90	70	29	190
TC89-31a#	41§	f	1.30	0.42	670	190	39	181	25	1160	60	70	355	90	70	25	180
TC89-28a#	37	f	1.37	0.54	1090	210	38	181	43	1900	50	45	425	80	50	24	140
TC89-27c#	34	f	1.22	0.37	470	180	40	194	18	1190	50	60	340	90	65	31	165
TC89-25a#	32	f	1.13	0.36	580	165	38	195	24	1330	50	40	330	75	60	31	155
TC89-24a#	31	f	1.34	0.51	890	220	39	187	44	1800	45	50	415	65	60	29	130
TC89-21b	30§	af	1.20	0.41	750	210	43	189	31	1470	55	40	400	85	60	28	170
TC89-21a#	30§	f	1.32	0.41	750	225	43	190	30	1340	55	60	370	75	60	29	155
TC89-19b#	29	f	1.01	0.36	530	150	37	210	29	1460	45	30	305	80	60	27	150
TC89-18a#	28	f	1.14	0.38	520	185	45	200	27	1220	55	50	295	90	60	29	160
TC89-17a#	27	f	1.11	0.45	710	165	33	198	39	1600	40	40	335	65	45	26	130
TC89-16a	26	f	1.00	0.37	390	165	40	217	25	1590	50	40	305	75	50	31	155
TC89-15#	25	f	1.00	0.36	360	145	40	218	22	1340	45	40	315	90	50	30	160
TC89-12#	24	f	0.92	0.35	120	170	48	227	7	930	50	60	215	90	65	37	180
TC89-20a#	18§	f	1.05	0.32	140	190	53	200	6	950	55	60	260	90	70	28	190
TC90-40	5§	f	1.03	0.35	30	160	49	267	<2	710	55	70	240	85	70	33	165
TC92-135	1	f	1.34	0.41	750	215	35	189	32	1270	55	55	375	90	65	26	175

Note: Numbers in square brackets are estimated standard deviations of analytical precision, multiple analytical runs (see Appendix B). See Table 1 for additional explanation.

*SNO = stratigraphic number.

†Sample types: af = ashflow tuff, nonwelded; f = fallout tuff; v = ash-flow tuff, basal vitrophyre.

§Tuff beds have been dated.

#Samples have been identified in distal sections.

glass with rather low Al_2O_3 concentrations (≈11.5%) and consistently low MnO concentrations (≈0.03%). The ratio of K_2O to Na_2O is moderately high (≈2) in these glass shards, but this is a reflection in part of exchange of K for Na in the glass during hydration and in part of Na loss under the electron beam during electron probe microanalyses. X-ray fluorescence analyses of minor and trace element concentrations show the glasses to be characterized by high concentrations of light rare earth elements (Ce averages ≈150 ppm) and moderate concentrations of Rb (150–270 ppm), Y (≈55 ppm), and Nb (≈40 ppm). The variable concentrations of Ba (30–1100 ppm) and Sr (1–55 ppm) are a strong indication that fractionation of sanidine and plagioclase feldspar was a major factor in generating the chemical variability measured in the glasses.

Like glass from the well-known Yellowstone eruptions, glass from the Trapper Creek tuffs generally falls within the Fe-Ca concentration range of G-type (gray type) rhyolitic glasses as defined by Izett (1981); that is, Fe > 0.55% and Ca < 0.55%. As seen by comparing analyses in Table 1 and Table 3, glasses in the most evolved (lowest Ba and Sr concentrations) of the Trapper Creek tuffs are most similar to the G-type glasses associated with major late Neogene pyroclastic units of the SRPVP such as the Huckleberry Ridge and Lava Creek ash

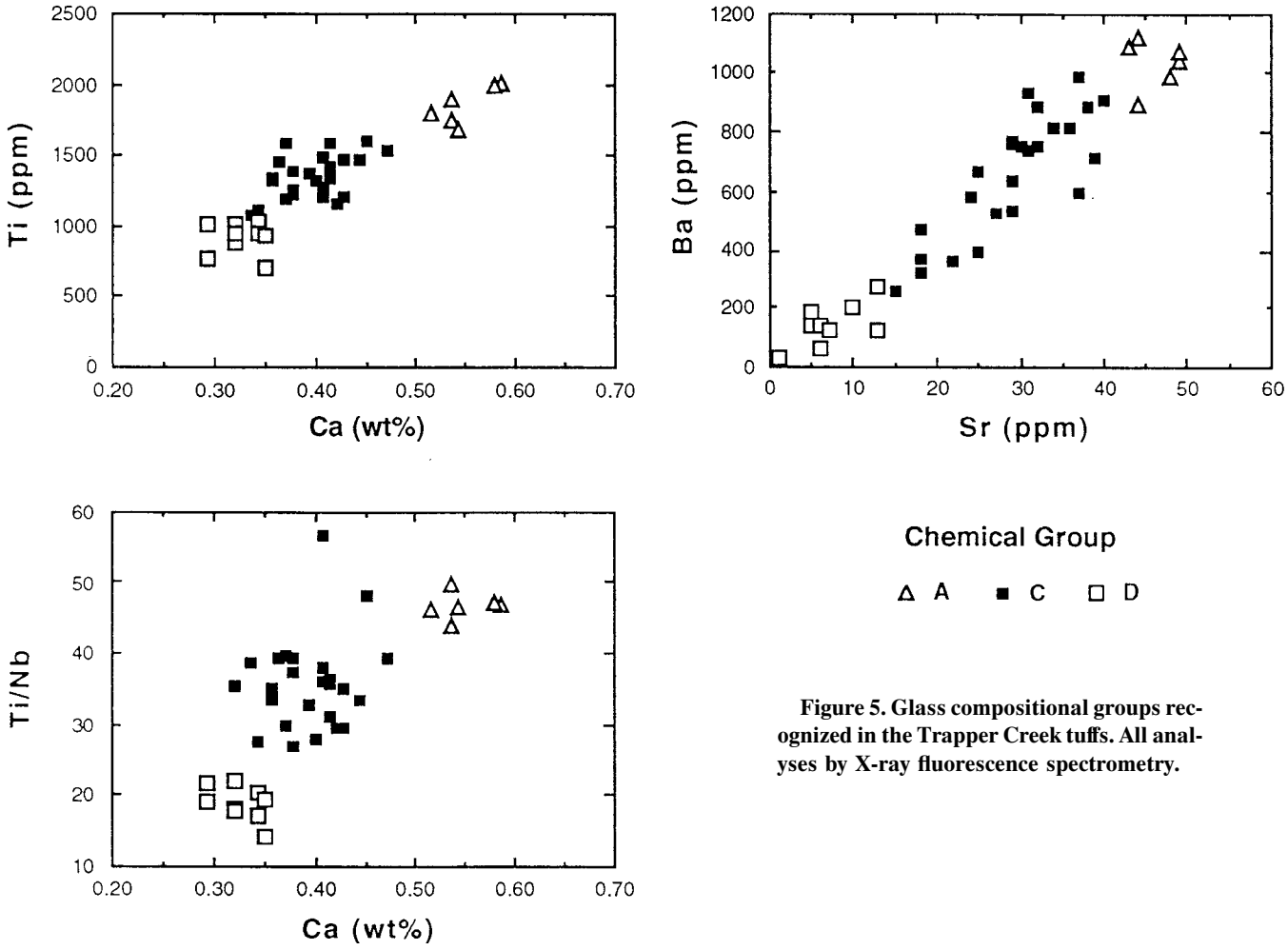

Figure 5. Glass compositional groups recognized in the Trapper Creek tuffs. All analyses by X-ray fluorescence spectrometry.

beds. The G-type glasses of Trapper Creek tuffs differ from the G-type glasses of pyroclastic units of the Jemez Mountains of New Mexico in having distinctly higher concentrations of Ca and Ti. This is evident in the comparison of the analysis of the Guaje ash bed (Table 1), a typical Jemez Mountain pyroclastic unit, with the analyses of Trapper Creek glasses.

Chemical Groups. Overall, glasses of the Trapper Creek tuffs vary almost continuously in composition, but, in detail, they tend to cluster into discernible chemical groups. Several possible groupings are suggested by the data, but a threefold chemical grouping of the glasses is convenient. These chemical groups, termed A, C, and D, are similar in most respects to the chemical groups A and F, C, and D, respectively, of Smith and Nash (1976). The group A glasses are the least evolved and contain high concentrations of Ba (>890 ppm), Sr (>42 ppm), and Ca (>0.5%), and low concentrations of Rb (<190 ppm) and Cl (≤0.03%). Tuffs with group A glass have little or no sanidine and often contain little or no quartz. The group D glasses are the most evolved and contain low concentrations of Ba (<300 ppm), Sr (<17 ppm), and Ca (<0.44%), and moderate concentrations of Rb (>190 ppm) and Cl (>0.05%). Tuffs with group D glass have high sanidine:plagioclase ratios and usually contain quartz. The group C glasses are mostly of intermediate composition between the group A and group D glasses. Tuffs with group C glasses generally have 10%–40% sanidine in the quartz/feldspar fraction, although some of the least evolved tuffs in this group have <5% sanidine. Chemical groups were identified using multivariate cluster analyses (Kaufman and Rousseeuw, 1990), but they are also discernible to some degree on bivariate plots (Fig. 5).

Multimodal Glass. Many of the tuffs in the Trapper Creek section contain glass shards with two or more compositional modes. This multimodality is revealed by electron probe microanalysis and is particularly evident on Ca versus Fe bivariate plots (Fig. 6). Bimodality is most common, but a number of tuffs contain three and even four distinct modes. Multimodality is most pronounced in the group A tuffs and the most Ba-rich of the group C tuffs. In these glasses the mode with the highest Fe concentration typically contains from 0.2 to 0.5 wt% more Fe than the mode with the lowest Fe concentration. Compositional differences between modes are less pronounced in tuffs with moderate to low Ba concentrations. The multimodality is not a result of post-eruption contamination, as it is observed in primary fallout tuffs. Further, ashflow tuffs with multimodal vitrophyres have basal fallout layers with similar multimodal patterns (Fig. 6), demonstrating that the multimodality is a primary magmatic feature reflecting heterogeneity in the magma reservoir. Finally, several multimodal Trapper Creek tuffs have been identified in Miocene basin fill deposits in western Nevada (Per-

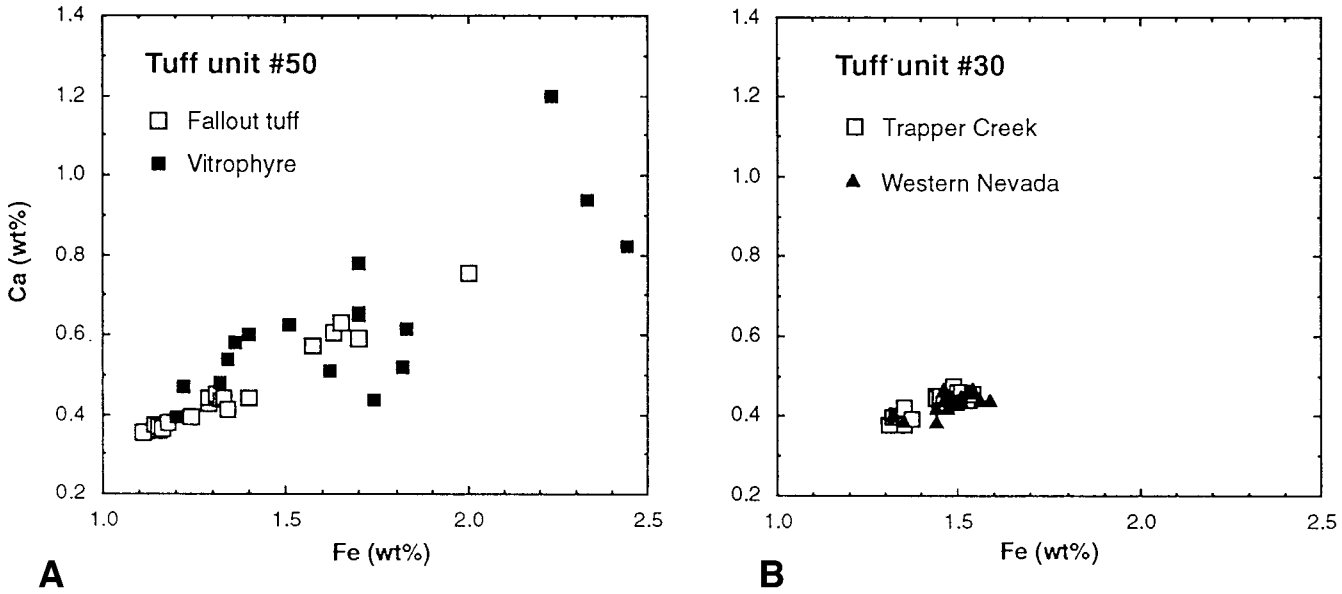

Figure 6. Multimodal glass shards in tuffs. Approximately 20 shards analyzed for each sample. (A) Glass shards in fallout tuff and glass in basal vitrophyre of overlying welded tuff. (B) Glass shards in fallout tuff of Trapper Creek section and correlative tuff in the Wassuk basin of western Nevada 500 km southwest of Trapper Creek.

kins, unpubl. data), further demonstrating that the multimodality is an essential characteristic of some eruptions and not an artifact of local sedimentary mixing of tuffs. One example of a regionally extensive multimodal tuff is shown in Figure 6.

Stratigraphic Variation of Tuff Composition

Stratigraphic variation in both mineralogy and glass composition is observed in the Trapper Creek tuffs. The most chemically evolved of the tuffs, group D, occurs only in the lower part of the section while the least evolved of the tuffs, group A, is restricted to the upper part of the section. The compositionally intermediate group C tuffs are concentrated in the central part of the section, but occur throughout. This up-section trend toward less evolved silicic tuffs is clearly reflected in the mineralogic and glass compositional trends. As seen in Figure 7, sanidine-rich (>40% of the quartz/feldspar fraction) tuffs occur only in the older part of the section (>12.5 Ma). At ca. 12.5 Ma there is a sharp drop in sanidine content, and after 12.5 Ma there is a general decline in sanidine content with tuffs younger than ca. 10.8 Ma having little or none. Incompatible elements, such as Rb, show stratigraphic variations similar to that of sanidine, while the compatible elements, such as Ba, show an up-section increase in concentration.

Two primary phases of silicic magmatism are recorded by the Trapper Creek tuffs: an older phase from 13.9 (or older) to ca. 12.5 Ma and a younger phase from ca. 12.5 to 8.6 Ma. The older phase repeatedly generated the very evolved group D tuffs along with some less-evolved group C tuffs. No strong compositional trends are evident during this early phase. The younger phase of silicic magmatism begins sharply at ca. 12.5 Ma as indicated by marked discontinuities or trend changes observed in the stratigraphic variation diagrams in Figure 7. In this later phase of magmatism, the earliest tuffs are relatively evolved, but later eruptions produced progressively less-evolved tuff, a trend that continues to the top of the section. As discussed in the next section, the compositional transition observed at ca. 12.5 Ma likely marks a change in the source of these tuffs.

SOURCES OF TUFFS

Clearly, explosive eruptions in the SRPVP generated the Trapper Creek (vitric fallout) tuffs. The glass fraction of these gray vitric tuffs shows strong chemical similarities to glass from major late Neogene pyroclastic deposits of the Heise and Yellowstone Plateau volcanic fields, which supports a SRPVP source for the older Trapper Creek tuffs as well. Further, the mafic silicates in silicic volcanic rocks of all types and ages from the SRPVP are almost always pyroxenes; biotite or hornblende are observed only rarely (Bonnichsen, 1982b, 1982c; Bonnichsen and Citron, 1982; Leeman, 1982a, 1982b; Ekren et al., 1984; Morgan et al., 1984; Honjo 1990), and pyroxenes are the only mafic silicates we have observed in either the fallout or ash-flow tuffs at Trapper Creek. In addition, the basal vitric fallout units associated with SRPVP ash-flow tuffs in the upper part of the Trapper Creek section provide a direct link of these fallout tuffs to SRPVP sources, and the near continuum of chemical and mineralogical variation between these upper fallout tuffs and the older fallout tuffs in the section indicates a SRPVP source for all the analyzed Trapper Creek tuffs. Finally, the SRPVP is the only silicic, middle–late Miocene volcanic province near enough and active enough to have repeatedly produced the thick layers of relatively coarse fallout tuff found in the Trapper Creek section. Other major provinces active during the 13.9–8.6 Ma time period are located in southern Nevada or in the volcanic plateau of central Oregon (Luedke and Smith, 1982, 1983). Such distal volcanic provinces are unlikely sources for either the thick fallout tuff or ash-flow tuff of the Trapper Creek section.

Three major volcanic fields of the SRPVP, the Owyhee-Humboldt, the Bruneau-Jarbidge, and the Twin Falls, were centers of explosive volcanism during the time vitric tuffs were accumulating at Trapper Creek

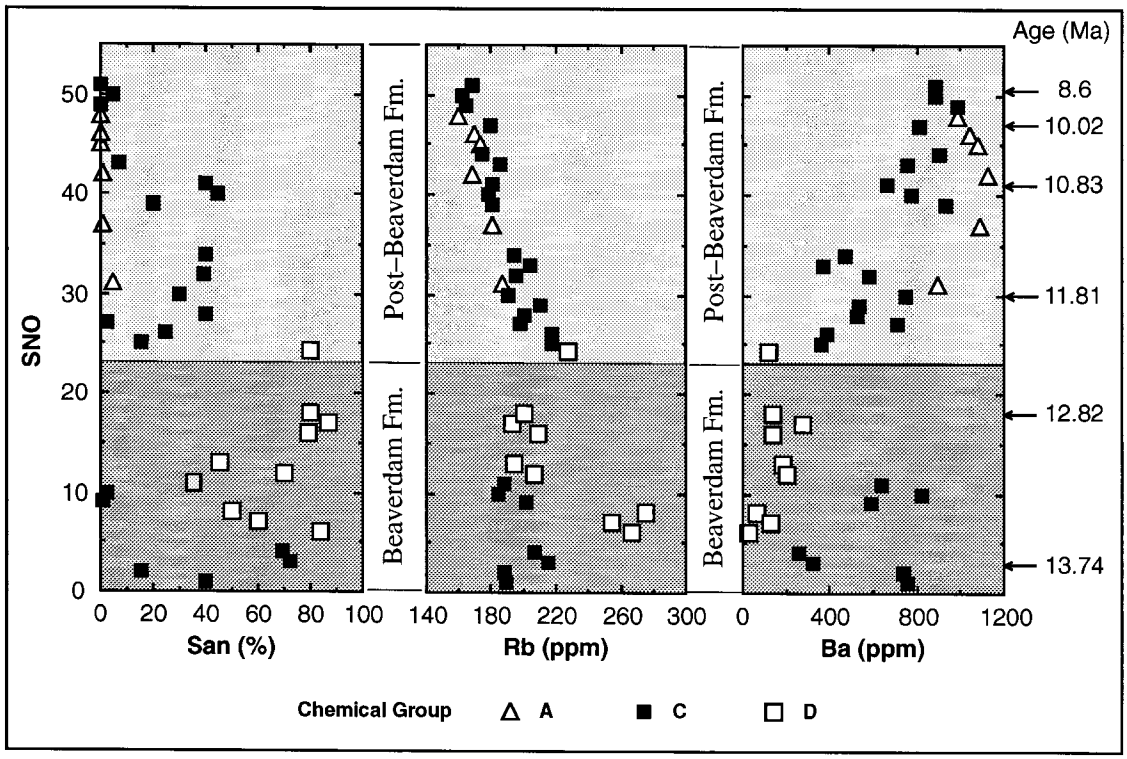

Figure 7. Stratigraphic variation in mineralogy and glass composition of the Trapper Creek (fallout) tuffs. San(%) = percentage sanidine in the quartz + feldspar fraction. SNO = stratigraphic number.

(Bonnichsen, 1982a; Ekren et al., 1984; Pearce and Morgan, 1992). To obtain more specific information on sources of the Trapper Creek tuffs, reconnaissance sampling was done along the southern margin of the Bruneau-Jarbidge volcanic field. Analyses of these samples, discussed below, indicate that many, if not all the tuffs in the middle part of the Trapper Creek section, were produced by eruptions in the Bruneau-Jarbidge volcanic field, while underlying tuffs may have had a source in the Owyhee-Humboldt volcanic field, and overlying tuffs may have had a source in the Twin Falls volcanic field.

Bruneau-Jarbidge Volcanic Field

A sequence of densely welded silicic ash-flow tuffs, named the Cougar Point welded tuff by Coats (1964), is widely exposed in the upper reaches of the Bruneau River and Jarbidge River around the southern margin of the Bruneau-Jarbidge volcanic field (Fig. 1). Bonnichsen and Citron (1982) describe nine separate ash-flow tuffs within the Cougar Point welded tuff, which they term units III, V, VII, IX, X, XI, XII, XIII, and XV from base to top. These ash-flow tuffs were erupted during the initial, explosive phase of the Bruneau-Jarbidge volcanic field according to these workers. An age estimate of 11.3 ± 2.0 Ma (K-Ar whole rock) is reported for the basal vitrophyre of Cougar Point tuff unit VII (Bonnichsen, 1982a), indicating that the Cougar Point tuff units are, in part at least, coeval with the Trapper Creek tuffs.

Eight of the Cougar Point tuff units (unit X not sampled) as well as a sequence of 10 gray, vitric, fallout tuffs beneath the Cougar Point tuff were sampled to assess possible correlations between these tuffs and the Trapper Creek tuffs. For the Cougar Point tuff units, basal fallout tuff was sampled when feasible. Units for which we found no exposures of basal fallout tuff include unit XIII and, in the Bruneau drainage, unit XV. Basal vitrophyre of the ash-flow tuff phase from these two units was sampled instead. Tuffs in the Bruneau-Jarbidge area are assigned stratigraphic numbers from 1 (base) to 20 (top) as shown on Figure 8. Differences in phenocryst abundance and glass composition suggest that Cougar Point tuff unit XV in the Bruneau drainage and Cougar Point tuff unit XV in the Jarbidge drainage are different units, here termed XV(b) and XV(j), respectively. For convenience, XV(b) is assigned stratigraphic number 19, and XV(j) is assigned stratigraphic number 20, but their stratigraphic position relative to one another is not known. As discussed below and shown in Figure 8, analyses of these Cougar Point tuff units provide firm evidence that the tuffs in the central portion of the Trapper Creek tuff sequence were generated by eruptions in the Bruneau-Jarbidge volcanic field and that the Cougar Point tuff units were emplaced in the period ca. 12.5 to ca. 10.0 Ma.

General Similarities to Trapper Creek Tuffs. Fallout tuffs in the Bruneau River and Jarbidge River canyon sections are similar in appearance and composition to the Trapper Creek tuffs and show similar stratigraphic variation in composition. As shown in Figure 9, tuffs exposed in these canyons generally fall within compositional ranges for groups A, C, and D, the three compositional groups encompassing the Trapper Creek tuffs. Further, stratigraphic variations in sanidine concentration and glass composition for the tuffs of the Bruneau and Jarbidge River canyons mimics the trends described for the Trapper Creek tuffs. As at Trapper Creek, the tuffs low in the section often have high proportions of sanidine and consist of a mix of tuffs with group C and D affinities that show no obvious stratigraphic trends in either mineralogy or glass composition. These tuffs are found in the sequence

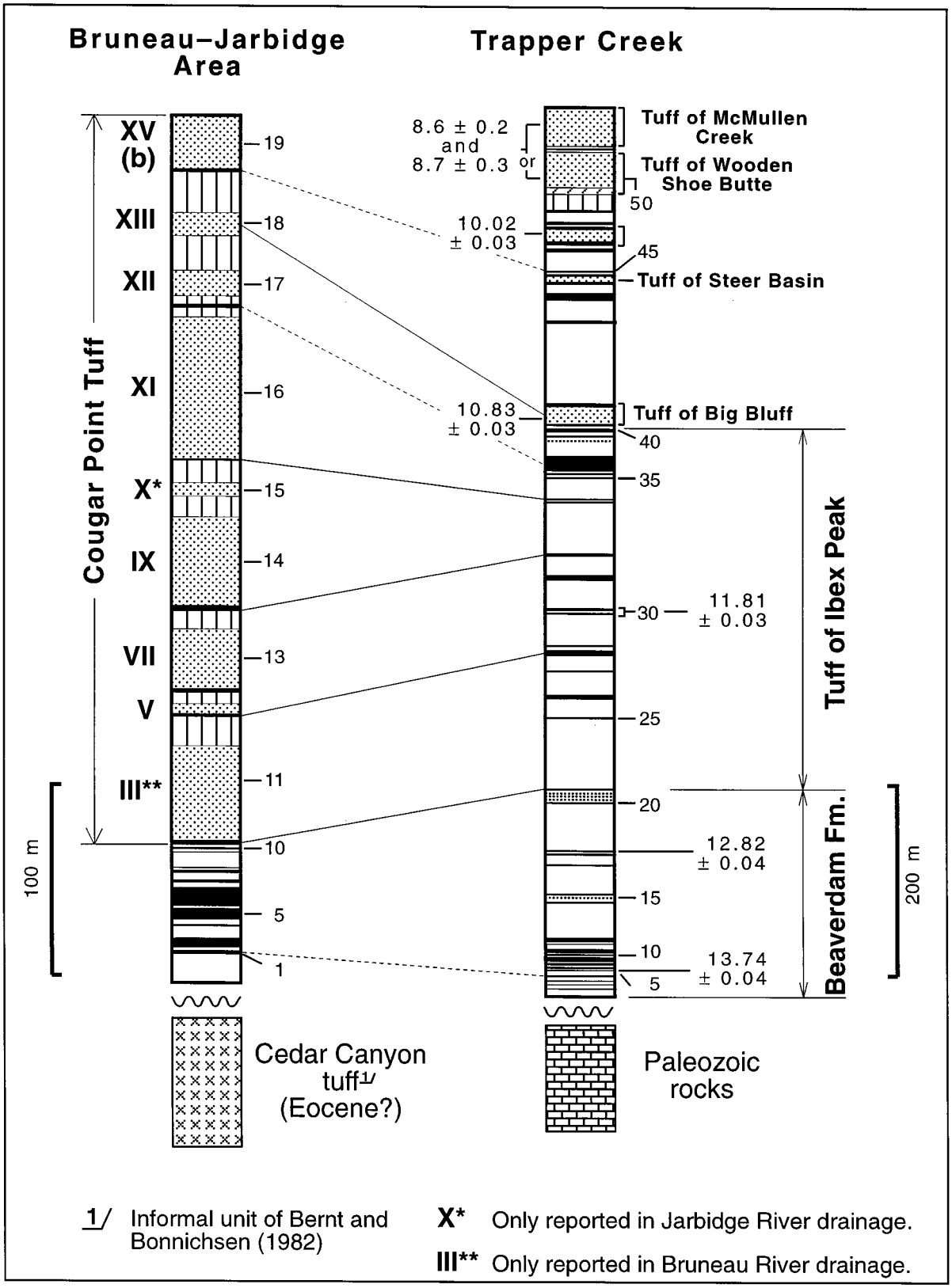

Figure 8. Correlation of tuffs in the Bruneau-Jarbidge area with tuffs in the Trapper Creek section. Solid lines for stronger correlations and dashed lines for weaker correlations. Thickness for Cougar Point tuff units primarily from the Bruneau River canyon. See Figure 3 for explanation of patterns and symbols.

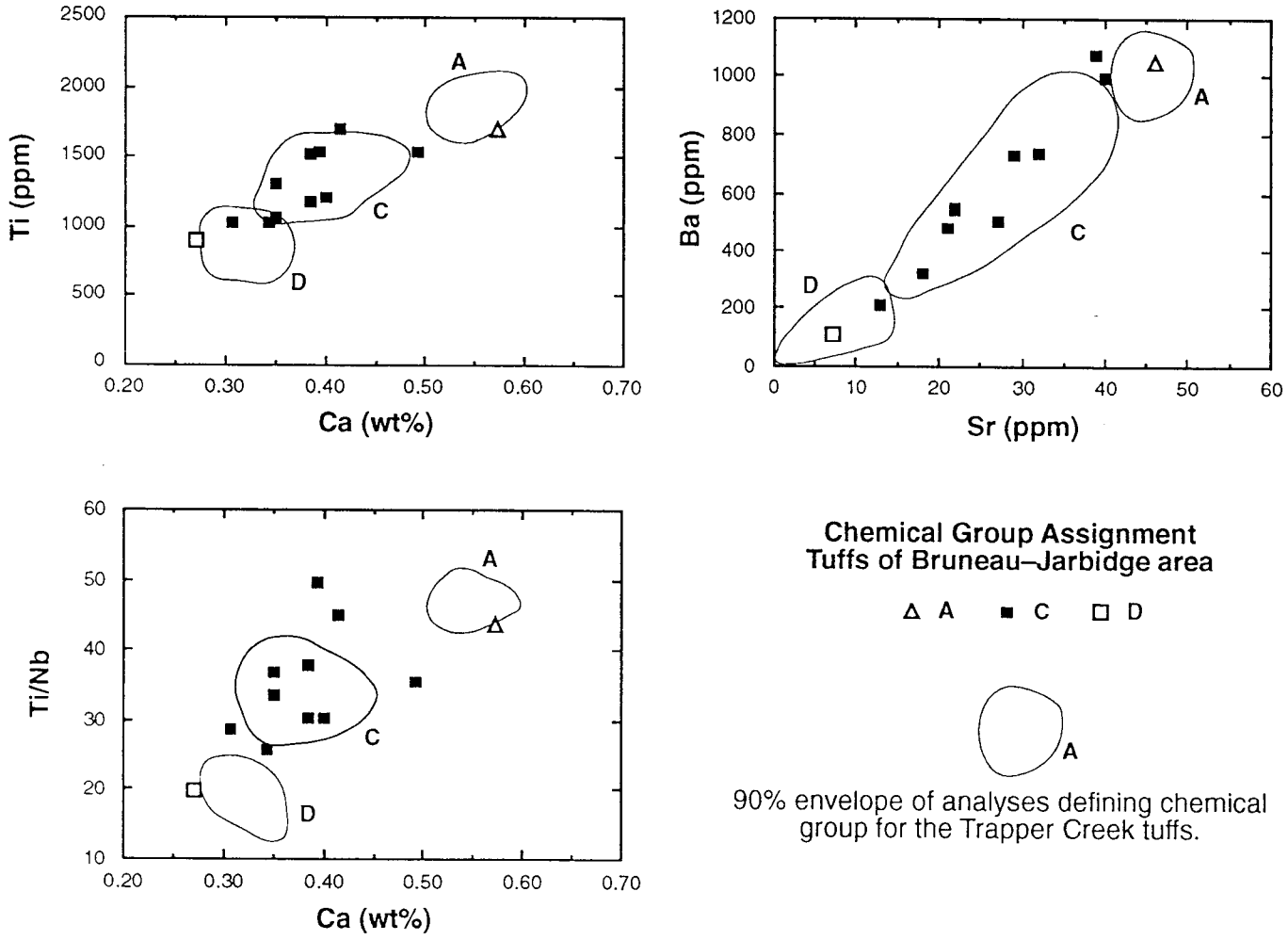

Figure 9. Chemical composition of glass in tuffs from the Bruneau-Jarbidge area. All analyses by X-ray fluorescence spectrometry.

of fallout tuffs beneath the Cougar Point tuff unit (Fig. 8). In contrast, most Cougar Point tuff units have generally moderate sanidine concentrations, consist of mostly group C tuffs (with one tuff each from groups A and D), and show a definite, up-section trend toward chemically and mineralogically less-evolved silicic tuffs as originally reported by Bonnichsen and Citron (1982). Thus the Cougar Point tuff units resemble the post-Beaverdam tuffs at Trapper Creek.

Bed-to-Bed Correlation with Trapper Creek Tuffs. Correlation of individual tuffs between the Bruneau-Jarbidge area and the Trapper Creek area confirms the general correlations discussed above. Our assessment of bed-to-bed correlations between these two areas is shown in Figure 8, with solid tie-lines representing the more convincing correlations between sections and dashed tie-lines representing potential correlations that need to be tested with additional information. Details regarding our approach to correlation of individual tuff units are discussed in Appendix B. The analyses of correlative or potentially correlative tuffs are given in Table 4.

Bed-to-bed correlations indicate that the explosive phase of the Bruneau-Jarbidge volcanic field began at 12.5 ± 0.2 Ma with the eruption of Cougar Point tuff unit III, a group D tuff, and ended at ca. 10 Ma with the eruption of Cougar Point tuff unit XV(b), a group A tuff. The age estimate for unit III is based on the average sedimentation rates between bracketing dated tuffs in the Trapper Creek section (Figure 4). The error estimate for this unit is based on work in progress, comparing such interpolated age estimates from section to section across the northern Basin and Range Province (Perkins et al., 1993). The age estimate for unit XV(b) is only approximate. Unit XV(b) is most similar to sample TC90-17 (stratigraphic number 45) at Trapper Creek but may not be correlative to this tuff (Table 4); however, unit XV(b) is a typical group A tuff, and the Rb concentration of its glass phase of ≈170 ppm indicates an age of ca. 10 Ma (Figure 7). Age estimates of other Cougar Point tuff units are as follows: unit V, 12.0 ± 0.2 Ma; unit IX, 11.5 ± 0.2 Ma; unit XI, 11.2 ± 0.2 Ma; and unit XIII (= tuff of Big Bluff), 10.83 ± 0.03 Ma. The Cougar Point tuff units represent a series of 9 to 10 chemically related, progressively less-evolved ash-flow tuffs erupted during a relatively brief time period of 2.5 m.y.

Likely Source of the 12.5–10.0 Ma Trapper Creek Tuffs. At Trapper Creek there are at least 23 separate fallout tuffs in interval 12.5–10.0 Ma (up to but not including tuff 47, the welded tuff dated at 10.02 Ma), all of

TABLE 4. COMPARISON OF ANALYSES OF GLASS OF CORRELATIVE/POTENTIALLY CORRELATIVE TUFFS

Sample	CPT* unit	SNO†	Type	Electron probe microanalyses														D#	SC#
				SiO_2 [0.5]	TiO_2§ [0.01]	Al_2O_3 [0.2]	Fe_2O_3§ [0.02]	MnO§ [.005]	MgO§ [.003]	CaO§ [0.01]	BaO [0.01]	Na_2O [0.2]	K_2O [0.1]	Cl§ [.002]	F [0.01]	H_2O [0.7]	–O [0.03]	Total [0.7]		
brv93-536	XV	b19	v	73.5	0.30	11.7	2.34	0.042	0.104	0.89	0.10	2.8	5.8	0.009	0.21	2.7	0.09	100.4		
ejr93-532b	XV?	b19j	v	73.5	0.27	11.5	2.54	0.038	0.057	0.74	0.12	2.8	5.8	0.029	0.25	2.8	0.11	100.3	18.4	0.74
ejr93-532a	XV?	b19j	f	73.5	0.28	11.5	2.49	0.043	0.058	0.75	0.11	2.3	6.6	0.023	0.18	3.1	0.08	100.9	3.0**	0.93**
tc90-17		tc45	f	72.6	0.32	11.6	2.33	0.029	0.123	0.80	0.10	2.5	5.7	0.027	0.25	5.0	0.11	101.3	10.1	0.78
brv93-537	XIII	b18	v	73.9	0.21	11.6	2.31	0.033	0.036	0.73	0.04	2.8	6.0	0.039	0.20	2.6	0.09	100.4		
tc89-33b		tc41	c	72.9	0.19	11.4	2.06	0.033	0.027	0.63	N.A.††	2.4	5.5	0.039	0.20	5.0	0.09	100.3	11.9	0.90
cks93-518a		cks	af	73.3	0.20	11.4	2.08	0.029	0.029	0.65	0.07	1.9	7.2	0.040	0.20	3.8	0.09	100.8	2.3**	0.95**
tc89-31a		tc41	f	73.1	0.21	11.4	2.10	0.030	0.027	0.65	0.08	2.7	5.5	0.043	0.27	5.2	0.12	101.2	9.9	0.89
cks93-518		cks	f	71.8	0.19	11.2	2.09	0.036	0.028	0.64	0.07	1.9	6.8	0.038	0.26	5.9	0.12	100.8	2.6**	0.93**
wjr93-538	XII	b17	f	73.2	0.31	11.7	2.25	0.026	0.126	0.77	0.12	2.7	5.8	0.023	0.31	2.5	0.13	99.7		
tc89-28c		tc37	f	72.5	0.31	11.5	2.16	0.033	0.114	0.74	0.11	2.5	5.6	0.023	0.30	4.3	0.13	100.1	5.1	0.93
tc89-28a		tc37	f	72.4	0.31	11.6	2.23	0.033	0.118	0.76	0.11	2.5	5.6	0.020	0.27	5.0	0.12	100.8	2.6	0.93
brv93-431a	XI	b16	wf	73.4	0.20	11.1	1.94	0.030	0.050	0.65	0.06	2.7	6.0	0.010	0.07	3.7	0.03	99.9		
tc89-27c		tc34	f	73.0	0.20	11.4	1.92	0.030	0.050	0.58	0.02	2.2	5.9	0.040	0.21	5.0	0.10	100.5	11.7	0.86
brv93-430	IX	b15	f	73.8	0.23	11.4	1.81	0.026	0.070	0.54	0.04	2.6	6.0	0.033	0.27	3.5	0.12	100.2		
tc89-25a		tc32	f	73.0	0.24	11.3	1.83	0.031	0.072	0.56	0.05	2.2	6.2	0.031	0.28	4.7	0.13	100.4	2.3	0.94
brv93-429	VII	b14	f	73.9	0.26	11.4	1.83	0.033	0.089	0.59	0.06	2.6	5.9	0.024	0.53	3.5	0.23	100.5		
tc89-21b		tc30	af	73.4	0.25	11.5	2.15	0.039	0.067	0.68	0.07	2.2	6.5	0.028	0.18	3.2	0.08	100.2	14.2	0.85
tc89-21a		tc30	f	72.7	0.25	11.3	2.10	0.030	0.058	0.61	0.09	2.1	6.3	0.031	0.28	5.1	0.13	100.8	5.9**	0.90**
brv93-427	V	b12	f	73.5	0.20	11.6	1.89	0.030	0.060	0.60	0.07	2.5	6.1	0.050	0.29	4.6	0.13	101.4		
wjr93-436	V	b12j	f	73.5	0.20	11.6	1.96	0.030	0.060	0.61	0.07	2.4	6.4	0.050	0.29	4.5	0.13	101.5	2.6	0.99
tc89-18a		tc28	f	73.3	0.20	11.5	1.88	0.030	0.060	0.59	0.07	2.3	6.2	0.050	0.28	5.3	0.13	101.6	0.8	1.00
brv93-432	III	b11	f	74.3	0.16	11.7	1.48	0.024	0.062	0.51	0.01	2.5	6.6	0.067	0.31	3.7	0.15	101.3		
tc89-14		tc24	f	73.2	0.15	11.5	1.47	0.026	0.061	0.52	0.00	1.8	6.8	0.069	0.33	6.1	0.15	101.9	1.4	0.96
tc89-13		tc24	f	73.5	0.15	11.6	1.45	0.024	0.057	0.51	0.01	2.1	6.3	0.071	0.33	6.1	0.15	102.1	2.3	0.96
tc89-12		tc24	f	73.6	0.14	11.6	1.46	0.028	0.056	0.50	0.01	2.2	6.2	0.071	0.33	6.1	0.15	102.1	2.8	0.92
tc92-143		tc24	f	73.1	0.15	11.5	1.44	0.019	0.050	0.50	0.01	1.6	7.0	0.073	0.32	6.0	0.15	101.6	4.0	0.90

Sample	CPT* unit	SNO†	Type	X-ray fluorescence spectrometry analyses														D#	SC#
				Fe§ [.03]	Ca§ [.02]	Ba§ [15]	Mn§ [4]	Nb [1]	Rb§ [3]	Sr§ [2]	Ti§ [25]	Y§ [2]	Zn [4]	Zr§ [8]	La [5]	Nd [5]	Th§ [2]	Ce [12]		
brv93-536	XV	b19	v	1.38	0.57	1050	220	39	171	46	1700	52	36	440	80	55	26	160		
ejr93-532b	XV?	b19j	v	1.55	0.49	1050	215	47	175	41	1940	59	68	460	90	70	25	155	10.4	0.92
ejr93-532a	XV?	b19j	f	1.50	0.48	1020	240	44	173	39	1610	59	63	460	85	70	24	160	7.8	0.92
tc90-17		tc45	f	1.43	0.54	1080	215	40	173	49	1750	50	47	485	75	55	27	150	5.0	0.96
brv93-537	XIII	b18	v	1.27	0.39	560	165	38	187	22	1160	75	59	360	90	65	29	150		
tc89-33b		tc41	c	1.29	0.41	590	180	40	186	23	1110	76	59	375	105	75	29	150	3.9	0.96
cks93-518a		cks	af	1.22	0.41	560	185	40	186	22	1210	75	60	360	90	55	29	170	4.2	0.97
tc89-31a		tc41	f	1.29	0.41	700	180	38	184	24	1120	76	63	350	95	60	30	185	7.4	0.95
cks93-518		cks	f	1.26	0.39	640	180	39	184	24	1100	74	59	340	90	60	23	155	4.1**	0.95**
wjr93-538	XII	b17	f	1.33	0.41	1000	195	38	178	40	1710	48	33	415	75	55	29	165		
tc89-28c		tc37	f	1.34	0.51	1000	205	39	184	39	1720	55	36	415	75	55	27	140	4.2	0.96
tc89-28a		tc37	f	1.37	0.54	1090	210	38	181	43	1900	48	46	425	80	50	24	140	7.1**	0.95**
brv93-431a	XI	b16	wf	1.14	0.39	480	185	39	191	21	1180	56	42	325	75	65	32	180		
tc89-27c		tc34	f	1.22	0.37	470	180	40	194	18	1190	52	59	340	90	65	31	165	3.0	0.96
brv93-430	IX	b15	f	1.13	0.35	540	165	39	199	22	1310	49	36	340	85	60	28	150		
tc89-25a		tc32	f	1.13	0.36	580	165	38	195	24	1330	49	38	330	75	60	31	155	2.8	0.96
brv93-429	VII	b14	f	1.16	0.39	740	205	40	199	32	1510	50	33	365	75	55	29	165		
tc89-21b		tc30	af	1.20	0.41	750	210	43	189	31	1470	54	40	400	85	60	28	170	4.9	0.96
tc89-21a		tc30	f	1.32	0.41	750	225	43	190	30	1340	54	61	370	75	60	29	155	6.0**	0.96**
brv93-427	V	b12	f	1.15	0.37	542	190	42	197	27	1080	65	40	300	85	65	26	165		
wjr93-436	V	b12j	f	1.14	0.36	556	195	41	195	29	1080	66	46	295	70	55	29	150	2.0	0.97
tc89-18a		tc28	f	1.10	0.36	506	185	43	197	25	1180	66	56	290	85	60	31	160	4.2	0.94
brv93-432	III	b11	f	0.89	0.27	109	140	46	232	7	910	51	47	240	95	60	34	195		
tc89-12		tc24	f	0.92	0.35	123	170	48	227	7	930	52	62	215	90	65	37	180	6.8	0.92
tc89-13		tc24	f	0.92	0.34	107	145	49	234	7	910	51	80	210	85	65	33	190	4.4	0.95
tc89-14		tc24	f	0.92	0.33	127	145	49	231	7	900	50	67	205	95	65	36	165	4.6	0.93
tc92-143		tc24	f	0.87	0.29	61	145	50	248	6	790	62	40	205	90	55	33	150	7.1	0.88

Note: Numbers in square brackets are estimated standard deviations of analytical precision, single analytical run (see Appendix B). See Tables 1 and 3 for additional explanation.

*CPT unit = Cougar Point welded tuff unit.

†SNO = stratigraphic number; b= Bruneau-Jarbidge area (with "j" indicating sample from Jarbidge River drainage); tc = Trapper Creek; cks= area halfway between Jarbidge River and Trapper Creek.

§Elements used in calculation of distance function (D) and similarity coefficient (SC).

#D = distance function; SC = similarity coefficient (see Appendix B).

**Values for comparison with sample in the row immediately above. Other values are for comparison with sample in first row of a group samples.

which are chemically similar to Cougar Point tuff units and all of which show the same stratigraphic variations in mineralogy and glass chemistry displayed by the Cougar Point tuff units. Because of these similarities, it is likely that most if not all of these 23 tuffs were generated by eruptions in the Bruneau-Jarbidge volcanic field and that, with respect to the number of preserved tuffs, the Trapper Creek section provides a more complete record of the explosive eruptions in this volcanic field than so far identified in more proximal sections. Fallout tuffs in the Trapper Creek section that are not correlated to specific Cougar Point tuff units are similar in all respects (glass composition, mineralogy, percentage of phenocrysts, glass shard morphology, and thickness) to the fallout tuffs that can be correlated to specific Cougar Point tuff units. Thus the inference is that these other tuffs are also the product of major explosive eruptions associated with the eruption of ash-flow tuffs in the Bruneau-Jarbidge volcanic field. There is some evidence of such additional units of Cougar Point welded tuff in the Bruneau-Jarbidge volcanic field. Bonnichsen and Citron (1982) note the presence of several probable ash-flow tuffs west of their study area that appear to be coeval with the Cougar Point tuff. Other such units may lie east of the better-studied portion of the Bruneau-Jarbidge volcanic field as noted by Bonnichsen (1981). Also, a large portion of the Bruneau-Jarbidge volcanic field is covered by rhyolite and basalt lava flows extruded after the eruption of Cougar Point tuff unit XV (Bonnichsen and Citron, 1982), thus other units of the Cougar Point tuff may lie buried beneath these lava flows. For these reasons we conclude that most if not all of the 12.5–10.0 Ma fallout tuffs at Trapper Creek were generated during major explosive eruptions in the Bruneau-Jarbidge volcanic field.

Conceivably, a few of the Trapper Creek tuffs were produced during the eruption of rhyolite lava from smaller, possibly coeval, volcanic centers identified in areas peripheral to Bruneau-Jarbidge volcanic field. These lavas do not appear to be interbedded with any ash-flow tuffs, according to Bonnichsen and Kauffman (1987). Their description of the lavas indicates that associated pyroclastic deposits are infrequent and limited to near-vent areas. This suggests that the eruptions producing these lavas were not generally associated with major explosive activity capable of repeatedly depositing thick ash blankets in the Trapper Creek area. Thus it is likely that few, if any, of the 12.5–10 Ma Trapper Creek fallout tuffs were produced during the eruptions of such rhyolite lava.

Owyhee-Humboldt Volcanic Field

The Owyhee-Humboldt volcanic field was the source of four major, middle Miocene silicic volcanic units named the Swisher Mountain Tuff, lower and upper lobes of the Juniper Mountain, and tuff of The Badlands (from oldest to youngest; Ekren et al., 1984). These units are typically rich in alkali feldspar phenocrysts. K-Ar dates on the three oldest units all average ca. 13.8 Ma, whereas the youngest unit has a K-Ar date of 12.0 ± 0.2 Ma (Ekren et al., 1984). These units were originally interpreted as very high-temperature ash-flow sheets (Ekren et al., 1984), but recent reevaluation of the characteristics of some of these units indicates they may be rhyolite lava flows (Manley, 1992). The age range and typically high alkali feldspar content of the silicic volcanic units of the Owyhee-Humboldt volcanic field make this volcanic field a possible source for the ca. 13.9–12.8 Ma group D tuffs of the Beaverdam Formation as well as similar age fallout tuff layers sampled in the Cedar Canyon section below Cougar Point Tuff unit III.

Both the group D and group C tuffs below Cougar Point tuff unit III are, on average, significantly thicker and coarser grained than similar tuffs in the Beaverdam Formation of Trapper Creek. This indicates a source nearer to the Bruneau River than to Trapper Creek, an observation compatible with a source in the general area of the Owyhee-Humboldt volcanic field. Further work is needed to assess the inference that the Owyhee-Humboldt volcanic field is the source of the older fallout tuffs of the Trapper Creek and Cedar Canyon sections, but available information supports this conclusion and suggests major explosive activity occurred in this volcanic field during the period ca. 13.9–12.8 Ma.

Twin Falls Volcanic Field

Pierce and Morgan (1992) observed that ash-flow tuffs in the ca. 11–8 Ma age range are broadly distributed in areas flanking the Snake River Plain at the approximate longitude of Twin Falls, Idaho. They infer, on the basis of this distribution pattern and their interpretation of unpublished gravity and magnetic data, that the source for these ash-flow tuffs is near Twin Falls, Idaho. The source vents/calderas within this proposed volcanic field, which they name the Twin Falls volcanic field, are entirely covered by later fill of the Snake River Plain downwarp. Pierce and Morgan (1992) assign the tuff of Steer Basin, the tuff of Wooden Shoe Butte, and the tuff of McMullen Creek to sources within their proposed Twin Falls volcanic field. The ca. 10.0–8.6 Ma ash-flow tuffs at Trapper Creek may have their source in this proposed volcanic field. These ca. 10.0–8.6 Ma ash-flow tuffs, as well as fallout tuffs interlayered with them, are the least evolved Trapper Creek tuffs—that is, the group A tuffs and the most Ba-rich of the group C tuffs—and a single source for these chemically similar tuffs seems reasonable. The few measurements we have made on the preferred orientation of lineations in the three uppermost ash-flow tuffs at Trapper Creek suggest a source in the northwest to northeast direction, that is, in the general direction of the proposed Twin Falls volcanic field.

DISCUSSION

The 51 vitric tuffs identified in the Trapper Creek, Idaho, section provide a sequential record of explosive volcanic activity within the Miocene part of the SRPVP. This record of explosive eruptions elucidates aspects of SRPVP volcanism that study of near-source ash-flow tuff and lava, the focus of all prior investigations of Miocene silicic volcanism within the SRPVP, has not fully addressed. In particular, the Trapper Creek tuffs provide (1) an estimate of the frequency of explosive eruption within the SRPVP for the period 13.9–8.6 Ma; (2) an estimate of temporal trends in silicic magma temperature for these eruptions; (3) information on chemical characteristics and age range of several proposed Miocene volcanic fields of the SRPVP and questions to pose about the definition of such volcanic fields; and (4) a basis for comparing and contrasting older with younger episodes of SRPVP silicic volcanism.

Frequency of Major Explosive Eruptions

Figure 10 shows fallout thickness versus age for the Trapper Creek tuffs and provides a basis for estimating eruption frequency, particularly frequency of major eruptions. Undated tuffs are assigned ages by linear in-

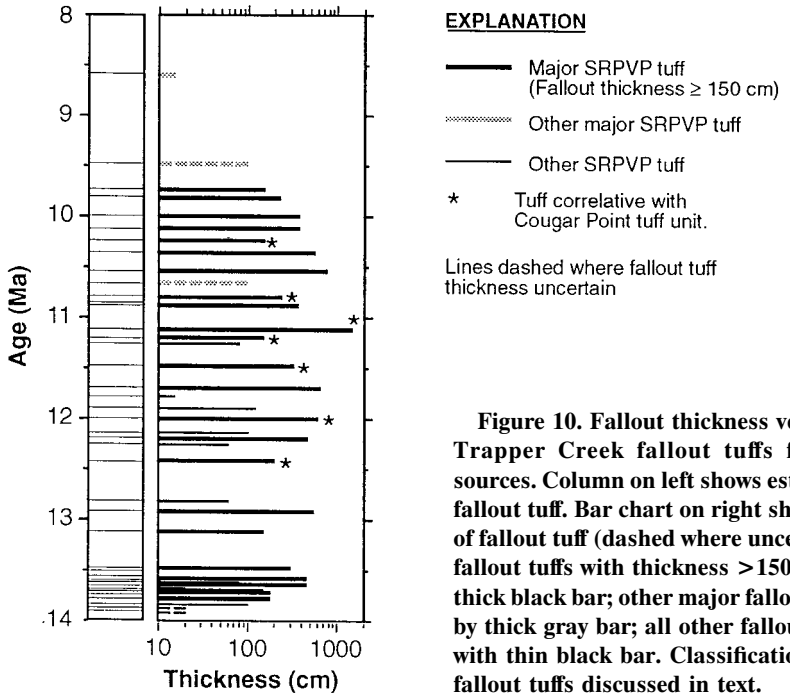

Figure 10. Fallout thickness versus time for Trapper Creek fallout tuffs from SRPVP sources. Column on left shows estimated age of fallout tuff. Bar chart on right shows thickness of fallout tuff (dashed where uncertain). Major fallout tuffs with thickness >150 cm shown by thick black bar; other major fallout tuffs shown by thick gray bar; all other fallout tuffs shown with thin black bar. Classification of "major" fallout tuffs discussed in text.

terpolation between dated tuffs; such ages appear reasonable judging from work on other correlative sections in the Basin and Range Province (Perkins et al., 1993). For discussion we define a "major" eruption as one that deposited 150 cm or more of fallout tuff at Trapper Creek, or is represented by a layer of reworked tuff ≥10 m in thickness, or is known to have an extensive ash flow associated with it. The five fallout tuffs that we can correlate with Cougar Point tuff units all satisfy one or both of the first two criteria for a major eruption. Thus, qualitatively, our definition of "major" is reasonable. It is also a conservative estimate, as thinner tuffs may well represent "major" eruptions in which prevailing winds deposited the thickest accumulation of fallout ash well away from the Trapper Creek area.

In all, there are 27 such major fallout tuffs among the 51 fallout tuffs in the Trapper Creek section. Of these, 22 have preserved fallout layers with thicknesses in the range 150–1500 cm, 4 lack preserved or exposed fallout tuff layers, but are represented by 10 m or more of reworked tuff, and one, the tuff of McMullen Creek, is an extensive ash-flow unit with a thin basal fallout tuff. Major fallout tuffs are distributed throughout the section with an average frequency of occurrence of about one major fallout unit per 200 k.y. (Fig. 10). There appear to be definite temporal variations in the average repose time between eruptions; however, how much of this variation is the result of vagaries in the completeness of the Trapper Creek record and how much represents actual variation in eruption frequency are unknown.

The estimated frequency for major eruptions should be considered a minimum as some observations indicate the Trapper Creek record of such eruptions is not complete. For instance, Nash et al. (1993), using data from a number of sections from throughout the Basin and Range Province, estimated about one explosive eruption per 80 k.y. during the time interval of the Trapper Creek section. Also, recall that of the eight major Cougar Point tuff units sampled in the Bruneau-Jarbidge volcanic field, only five have been positively identified at Trapper Creek. This suggests the Trapper Creek record is ≈60% complete for major eruptions from this volcanic center. This record may well be less complete for major eruptions in the more distant Owyhee-Humboldt volcanic field and more complete for major eruptions in the nearby Twin Falls volcanic field.

Size of Major Explosive Eruptions

While only qualitative estimates can be made for the size of the major eruptions recorded in the Trapper Creek section, each likely generated 50–1000 km^3 of uncompacted, widely distributed fallout tuff. The eruptions associated with these major fallout tuff layers were almost certainly larger, on average, than the eruptions that produced the well-documented Holocene Mazama and White River (east lobe) ash beds of North America (Bacon, 1983; Lerbekmo et al., 1975). These Holocene ash beds have estimated uncompacted volumes of ≈110 and 15 km^3, respectively, and deposited 15 and 70 cm, respectively, of uncompacted fallout ash at a distance of 100 km from the source—that is, the distance from the Bruneau-Jarbidge volcanic field to Trapper Creek. There is little available fallout thickness distribution data on larger explosive silicic eruptions, but Rose and Chesner (1987) suggest that the 75 ka Toba eruption produced 750 km^3 (observed) to 1700 km^3 (calculated) of uncompacted fallout ash. Data of Ninkovich et al. (1978) suggest that the Toba eruption deposited 100–200 cm of fallout ash 100 km downwind of its source caldera in Sumatra. Ongoing work on the regional distribution of Miocene fallout tuff from the SRPVP (Perkins et al., 1993, 1995) indicates that the more extensive of these tuffs blanketed large parts of the western United States. Thus they may have been produced by eruptions comparable in size to those that generated the well-documented Huckleberry Ridge and Lava Creek ashes (Izett and Wilcox, 1982). The Trapper Creek tuffs that are known to extend well beyond the SRPVP are flagged with an asterisk on Figure 3.

Magma Temperatures and the Cougar Point "Flare-up"

The occurrence of relatively high-temperature, Miocene ash-flow tuffs and lavas within the SRPVP has been reported by a number of workers. Hildreth (1981) reports Fe-Ti oxide temperatures in the range of 960–1030 °C for the Cougar Point tuff (ash-flow) units. Hackett et al. (1989) described features of densely welded tuffs in the central part of the SRPVP that they attributed to very high emplacement temperatures (>950 °C). Honjo et al. (1992) used feldspar, pyroxene, and Fe-Ti oxide geothermometry to estimate magma temperatures for 27 samples of Miocene silicic ash-flow tuff and lava from the central and western SRPVP. They report estimated temperatures >900 °C for most of their samples. Ekren et al. (1984) reported Fe-Ti oxide

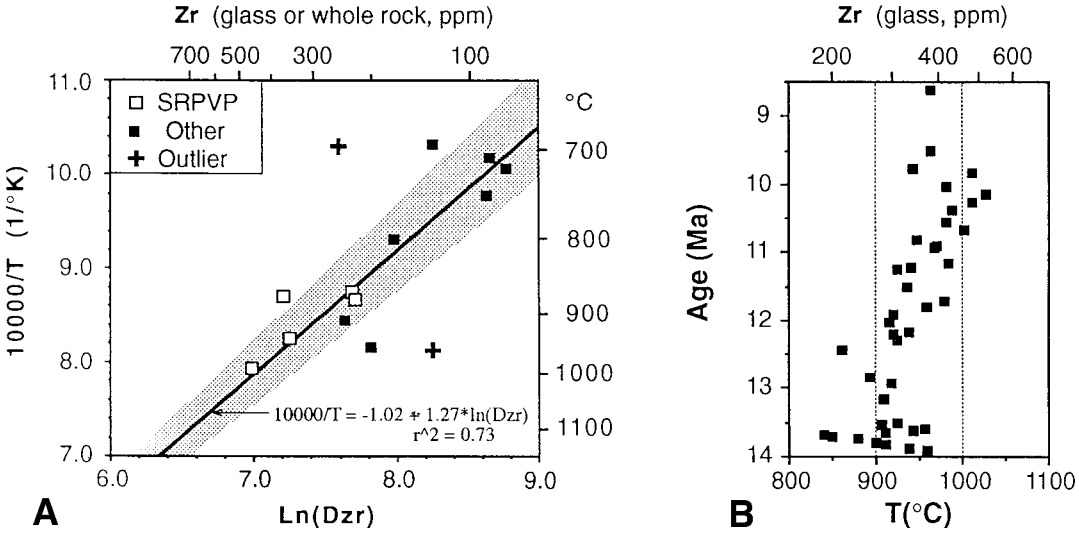

Figure 11. Estimated magma eruption temperatures of fallout tuffs. (A) Comparison of 1/T versus ln(D_{zr}) best-fit line and 50 °C envelope shown; (B) age versus estimated eruption temperatures for the Trapper Creek (fallout) tuffs. Temperature data from Bacon and Duffield (1981); Duffield and Ruiz (1992); Honjo et al. (1991); Izett (1981); Warshaw and Smith (1988). Zr concentrations in glass are from SRPVP samples in this study, from our unpublished data, or from the above references. Samples excluded from the linear regression include Guaje ash (≈700 °C, 220 ppm Zr) and sample OL-4 of the Los Chocoyos ash (≈960 °C, 130 ppm Zr).

temperatures of ≈1100 °C for silicic volcanic units in the western part of the SRPVP, but results of later studies (Honjo et al., 1992; Manley, 1992) indicate lower eruption temperatures (800–960 °C) for these units. Bonnichsen (1982b) reported on a number of features of the Cougar Point tuff units suggesting high temperatures during emplacement. While most of the reported high-temperature silicic tuffs or lavas are in the ca. 11–9 Ma age range, little detailed information is available on the pattern, if any, of temporal variation of magma temperature for Miocene silicic volcanic rocks of the SRPVP. Insight into the temporal pattern of magma temperature is provided by the Trapper Creek tuffs. As discussed below, zirconium concentration in glass can be used to estimate magma temperature, and, hence, the variation of magma temperature with time can be estimated using our analyses of zirconium concentration in glass from the Trapper Creek tuffs.

As discussed by Watson and Harrison (1983), the concentration of zirconium in silicic melts containing zircon (that is, saturated in Zr) is a function of temperature and melt composition. The function, as shown by theoretical calculations and experiments they performed is,

$$\ln(D_{zr}) = a + b/T,$$

where $D_{zr} = Zr_{zircon}/Zr_{glass}$, a = a function of the molecular ratio (Na + K + 2Ca)/(Al * Si), and b = a constant. For high-silica glass, such as that found in the Trapper Creek tuffs, (Na + K + 2Ca)/(Al * Si) is nearly constant at ≈0.8, so it is possible to estimate temperature by calibrating the ln(1/Zr) versus 1/T relationship. Such a calibration is shown on Figure 11A, which plots Zr concentrations in high-silica glass against reported magma temperatures as determined by Fe-Ti oxide or pyroxene geothermometry for 14 high-silica, rhyolitic glasses. Excluding two clear outliers, the regression line for these data is well defined (regression coefficient = 0.73), with most points falling within 50 °C of this line. Since the data sources for Figure 11A are varied, some of the data scatter is likely the result of variation in calibration of Zr concentration between various laboratories. Outliers may be glasses that are not saturated with respect to Zr.

This ln(D_{zr}) versus 1/T relationship provides a rough geothermometer for the Trapper Creek tuffs. The Zr_{glass} temperature estimates for these tuffs indicate that magmas erupted before 13 Ma averaged ≈900 °C but with a considerable range in temperature (840–960 °C) for individual eruptions (Fig. 11B). After 13 Ma the temperature range is narrower (≈60 °C) at any given horizon, and there is a well-defined up-section trend toward higher temperature magma, which culminated in the eruption of high-temperature magmas (≈1000 °C) during the interval 10.5–9.5 Ma. We term this well-defined Miocene trend toward eruption of higher temperature magma the Cougar Point "flare-up," because fallout layers from the eruption of Cougar Point tuff units are among the more prominent units associated with this magma temperature trend. This trend reflects the earlier observation by Bonnichsen (1982c) of an up-section progression toward less evolved silicic ash-flow tuffs in the Bruneau-Jarbidge volcanic field. After 9.5 Ma a slight decline in magma temperature is suggested by the decline of Zr in glass of the capping tuffs at Trapper Creek (Fig. 11B).

Miocene Volcanic Fields of the SRPVP

In the previous discussion, the Trapper Creek tuffs were assigned sources within three of the four volcanic fields of the SRPVP that Pierce and Morgan (1992) proposed were active during the interval from 13.9–8.6 Ma. While such an assignment appears reasonable and is in agreement with current concepts of location and age range of the principal sources within the Miocene SRPVP, the chemical and mineralogical characteristics of the Trapper Creek tuffs permit alternate interpretations.

The tuffs assigned to the Humboldt-Owyhee volcanic field include two distinct types, group D and group C tuffs, with little indication of tuffs of intermediate composi-

tion in this oldest group of Trapper Creek tuffs. The same pattern is observed for the fallout tuffs underlying the Cougar Point welded tuff in the Bruneau-Jarbidge area. While it is entirely possible that a single volcanic field could produce tuffs of two distinct compositions, the alternate possibility should be considered: that two separate but coeval volcanic fields were the source of the two different types of tuff assigned to the Owyhee-Humboldt volcanic field. For much of the region encompassed by the Owyhee-Humboldt field only the most basic reconnaissance information is available, so this alternate possibility cannot yet be tested.

The Cougar Point tuff units and coeval tuffs in the Trapper Creek section consist primarily of tuffs with group C glass. These tuffs and a few associated group A and group D tuffs have been assigned to the Bruneau-Jarbidge volcanic field following the suggestion of Bonnichsen (1982a) that his Cougar Point tuff units originated within this volcanic field; however, there is no direct evidence, such as isopach maps or flow direction indicators, that uniquely ties all units of the Cougar Point tuff to the Bruneau-Jarbidge volcanic field (Fig. 1). The identification of the ash-flow facies of Cougar Point tuff unit XIII far to the east in the Trapper Creek area indicates the great mobility of some of the Miocene ash flows and points out the need to map the distribution of individual ash-flow units before reaching a final assessment on ash-flow sources. The distinctive group D-type Cougar Point tuff unit III, the oldest unit of the Cougar Point tuff, could conceivably have had its source in the Owyhee-Humboldt volcanic field as has been suggested for all the underlying group D tuffs. Similarly, the group A-type Cougar Point tuff units XV(b) and XV(j), youngest in sequence comprising the Cougar Point tuff, may have had a source in the Twin Falls volcanic field where other overlying group A tuffs in the Trapper Creek section appear to have originated.

A final consideration is a possible close tie between what are currently regarded as two discrete volcanic fields, the Bruneau-Jarbidge and Twin Falls volcanic fields. As discussed previously, no clear break in either phenocryst or glass compositional trends is evident in the post-12.5 Ma tuffs of Trapper Creek. If the Bruneau-Jarbidge and Twin Falls volcanic fields are really two discrete volcanic fields separated by ≈100 km, as suggested by Pierce and Morgan (1992), we would anticipate some observable discontinuity in the composition of tuffs as volcanism shifted to the younger Twin Falls field. Perhaps the Bruneau-Jarbidge and Twin Falls volcanic centers mark the endpoints of a series of eruptive centers active during the interval 12.5–8.6 Ma.

Additional studies will be necessary to locate sources of individual pyroclastic eruptions and test the validity of proposed Miocene SRPVP volcanic fields. Tracing the distribution pattern of ash-flow tuffs and associated fallout tuffs will provide important evidence for source location. The study of the Trapper Creek tuffs indicates that glass composition, particularly of the generally unaltered fallout tuffs, can be used to identify individual pyroclastic units.

Comparison with Younger Explosive Volcanic Activity Within the SRPVP

Ideas on the nature of silicic volcanism throughout the SRPVP are influenced strongly by work on the best exposed and most intensively studied part of this province, the latest Neogene and Quaternary Yellowstone Plateau volcanic field. As summarized by Christiansen (1984), major explosive eruptions within this volcanic field are rare events. They have occurred on average about once every 600 k.y. during the past 2 m.y., with each eruption producing immense volumes (280–2500 km^3) of pyroclastic material. The magma erupted during these events was of a relatively moderate temperature, 860 °C on average for the Plinian fallout tuffs and basal units of the ash-flow tuffs (Hildreth, 1981; Izett, 1981). These major eruptions were associated with the formation of elliptical, nested calderas up to 90 km in length. Between the major pyroclastic eruptions, volcanic activity consisted primarily of the quiet eruption of basalt and rhyolite flows around the periphery and interior of these calderas. Together, the calderas and associated ash-flow tuff, rhyolite, and basalt form a geographically restricted, genetically linked entity that can be well described as a volcanic field. From mapping and correlation of individual ash flows, and interpretation of geophysical anomaly patterns, Morgan et al. (1984) have concluded that a similar pattern of infrequent eruption of extensive ash-flow tuffs linked to large, overlapping caldera sources characterized the silicic volcanism associated with the latest Miocene–Pliocene Heise volcanic field located in the eastern Snake River Plain. Three major ash-flow tuffs (tuff of Blacktail Creek, Walcott Tuff, and tuff of Kilgore), two more localized ash-flow tuffs (tuff of Wolverine Creek and Conant Creek Tuff), and some associated rhyolite and basalt flows are currently included in the Heise volcanic field (Morgan, 1992; Morgan et al., 1984). These tuffs erupted during the period from 6.5 to 4.3 Ma for an average of one ash-flow tuff-forming eruption about every 500 k.y. Estimated volumes of major eruptions are in the range of 1000–1500 km^3 (Hackett and Morgan, 1988). The Zr concentration in the glass of these ash-flow tuffs and associated fallout tuffs is low, 200–275 ppm, and similar to that of the major pyroclastic eruptions of the Yellowstone Plateau volcanic field (Table 1). Thus the pattern of infrequent eruption of major ash-flow tuffs from moderate temperature magmas (≈860 °C) appears to characterize the explosive silicic volcanism within the SRPVP during the past ≈7 m.y.

Clearly, this pattern contrasts with the pattern in older volcanic fields of the SRPVP of relatively frequent eruption (about one major event per 200 k.y.) of often relatively high-temperature silicic magma that we have documented in the investigation of the Trapper Creek tuffs. This change in style of explosive volcanism occurred during the period ca. 9.5–6.5 Ma, a time when the locus of SRPVP silicic volcanism moved eastward from the general area of the proposed Twin Falls volcanic field into the area of the Heise volcanic field within the eastern Snake River Plain. Factors contributing to this change in style of explosive silicic volcanism may include one or more of the scenarios described in the sections that follow.

Change in Crustal Structure. Prior to modification by SRPVP magmatism, several generally north-trending crustal boundaries or lithotectonic belts traversed southern Idaho. Of particular significance may be the western edge of the Precambrian basement. This boundary, now largely buried beneath Phanerozoic strata is likely near the Sr_i = 0.706 line or the nearly coincident ε_{ND} = −7.0 line (Farmer and DePaolo, 1983). The Sr_i = 0.706 line appears to have crossed the SRPVP between long 116°W and 117°W (Farmer and DePaolo, 1983; Leeman et al., 1992), that is, in the vicinity of the Owyhee-Humboldt volcanic field (Fig. 1), although results of Elison et al. (1990) suggest that the Sr_i = 0.706 line may cross southern Idaho as far east as long 114°W. Deep-seated crustal fractures associated with this

Precambrian rift boundary could facilitate intrusion of basaltic magma into the crust and enhance generation of silicic magma by partial melting of crustal rocks. Other crustal features that may have influenced SRPVP magmatism include the axis of the late Mesozoic magmatic arc (Coney, 1978); the belt of crustal thickening, metamorphism, and magmatism associated with the late Mesozoic Sevier orogeny (Coney and Harms, 1984) eastward of the magmatic arc; and the belt of extreme Tertiary extension and associated metamorphic core complexes within the central part of the Cordillera (Armstrong and Ward, 1991).

Change in Rate of Extension. Assuming the SRPVP volcanism is driven by a stationary mantle hot spot, analyses of the rate of eastward migration of this volcanism indicate that rates of extension along the hotspot track were substantially higher during the eruption of the Trapper Creek tuffs (≈4 cm/yr) than during later phases of SRPVP volcanism (≈1 cm/yr) (Pierce and Morgan, 1992; Smith and Braile, 1993). Higher extension rates could have contributed to the more vigorous rate of explosive volcanism documented by the Trapper Creek tuffs by facilitating the intrusion of mantle-derived basalt into the crust. A higher flux of basalt into the crust would enhance partial melting of the crust, and the fracturing associated with higher rates of extension could provide more pathways for these silicic melts to reach the surface. A higher flux of basalt into the crust could also generate the higher temperature magma that erupted during the Cougar Point "flare-up."

Change in Mantle Hot Spot. Pierce and Morgan (1992) emphasize that changes in the structure of the proposed mantle hot spot beneath the SRPVP may provide an explanation for changes in the distribution pattern of SRPVP eruption centers. In the early stages of its development the SRPVP sources appear to be broadly distributed, but between ca. 10 and ca. 7 Ma they become tightly focused within the confines of the present eastern Snake River Plain downwarp. Pierce and Morgan (1992) propose that the initial broad distribution of eruption centers reflects the initial interaction of the broad and voluminous head of the mantle plume with the continental lithosphere. Later, as SRPVP volcanism migrated into the eastern Snake River Plain region, the plume head had dissipated and the narrow tail of the plume provided a focused heat source that generated the youngest volcanic fields of the SRPVP. The larger head phase of the plume conceivably generated greater volumes of basaltic magma which, in turn, lead to widespread melting of the lower crust and the high frequency of explosive silicic volcanism documented at Trapper Creek. The reduced level of eruption activity since ca. 7 Ma by this scenario reflects a decrease in the volume of basaltic magma and a more restricted melting of the lower crust.

Clearly, the above are only some possible factors that may influence the temporal change in style of explosive volcanism indicated by the analyses of the Trapper Creek tuffs. The generation and eruption of explosive magmas is a complex process. The sequence of tuffs at Trapper Creek documents some of the changes occurring in the SRPVP. Future investigations can focus more closely on the nature of these changes and the factors that may contribute to them.

CONCLUSIONS

The Trapper Creek tuffs provide a sequential record of explosive silicic volcanism within the Snake River Plain volcanic province during the Miocene. Dating of the tuffs demonstrates that vigorous explosive volcanism within this major volcanic province was underway by ca. 13.9 Ma and continued unabated until 8.6 Ma, the period covered by the Trapper Creek record. Correlating tuffs of the Trapper Creek section with those of the Bruneau-Jarbidge area indicates that the explosive phase of the Bruneau-Jarbidge volcanic field occurred in the period 12.5–10.0 Ma. Older Trapper Creek tuffs may have had sources in the Owyhee-Humboldt volcanic field, while younger tuffs, including welded ash-flow tuffs, were likely from the general area of the proposed Twin Falls volcanic field. During the accumulation of the Trapper Creek tuffs there were changes in the composition of the silicic magmas being erupted from the SRPVP. These changes included distinct shifts in magma composition as the center for SRPVP volcanism shifted eastward to younger volcanic fields and also more gradual changes in composition accompanying a progressive increase in magma temperatures during the period from 12.5 to 9.5 Ma. In general, when compared to the latest Miocene and younger SRPVP volcanism, rates of explosive eruption were two to three times higher during the accumulation of the Trapper Creek tuffs, and the temperature of erupted silicic magma was higher on average, with highest estimated temperatures occurring around 10 Ma with the eruption of silicic magma at ≈1000 °C.

ACKNOWLEDGMENTS

We thank Andrei Sarna-Wojcicki for his interest and support in obtaining high-precision age dates for the Trapper Creek tuffs. We also thank John Bernt for discussing with us his ideas on the SRPVP volcanism and for showing us several key exposures near Jarbidge, Nevada. The assistance of Steve Williams in the preparation and X-ray fluorescence analysis of samples is most appreciated. James Saburomaru assisted with $^{40}Ar/^{39}Ar$ laser-fusion age determinations. Reviews of a draft manuscript by Bill Bonnichsen, Curtis Manly, Andrei Sarna-Wojcicki, and Brent Turrin were helpful and contributed to improvements in this manuscript. This work was supported by National Science Foundation grants EAR 9204700 and EAR 9316289 and by the Mineral Leasing Fund of the State of Utah.

APPENDIX A: DESCRIPTION/LOCATION OF DATED SAMPLES AND MEASURED SECTIONS

Samples

TC90-20/92. Basal vitrophyre of a 9-m-thick welded ash-flow tuff. Dark brown, slightly welded vitric tuff with 5%–10% phenocrysts consisting of 80%–90% plagioclase, 5%–15% quartz, 2%–5% sanidine, 1% Fe-Ti oxides, and trace of clinopyroxene. Collected along north side of Trapper Creek road 555 m west of east line and 884 m south of north line, sec. 26, T. 14 S., R. 21 E.; Oakley, Idaho, 7.5′ quadrangle; long 114°57.77′W, lat 42°10.64′N.

TC89-32/92. Upper vitrophyre of a 15-m-thick welded ash-flow tuff mapped as the tuff of Big Bluff by Mytton et al. (1990). Vitrophyre consists of 3 m of black perlitic obsidian with abundant spherulites in basal 1 m. Contains ≈5% phenocrysts consisting of 30%–40% sanidine, 20%–30% plagioclase, 25%–35% quartz, 10% perthitic feldspar (xenocrystic?), 1%–2% Fe-Ti oxides, and a trace of zircon. Collected in an area of rugged outcrops at the head of drainage east of Ibex Hollow, 76 m north of south line and 716 m west of east line, sec. 12, T. 15 S., R. 20 E.; Severe Spring, Idaho, 7.5′ quadrangle.; long 114°03.30′W, lat 42°07.72′N.

TC89-21B/92. Sample from the central part of a dark grayish brown, nonwelded, vitric ash-flow tuff. This ash-flow tuff is a local unit found in the upper part of a 30-m-thick channel fill complex exposed in the middle part of the tuff of Ibex Peak. The tuff forms a prominent dark outcrop in a rugged area of cliffs and badlands at the head of a side canyon that drains into Ibex Hollow. Contains ≈5% phenocrysts consisting of 30%–40%

plagioclase, 15%–25% quartz, 5%–10% sanidine, and 1%–2% Fe-Ti oxides. Collected along a fence line 229 m south of north line and along west line, sec. 13, T. 15 S., R. 20 E.; Severe Spring, Idaho, 7.5′ quadrangle; long 114°04.08′W, lat 42°07.55′N.

TC89-20A. Sample from the base of a friable, light gray, fallout/reworked vitric tuff. This is the uppermost, prominent tuff in the Beaverdam Formation of Axelrod (1964). The tuff is ≈2 m thick where sampled and includes a 0.0- to 0.6-m-thick laminated fallout tuff at the base, which is overlain along an erosional contact by 1–2 m of reworked, cross-bedded tuff. The tuff lies on a 0.5-m-thick lignite mapped as the Grant zone lignite by Mapel and Hail (1959). Old workings of this lignite near the sample location are identified as the Smith prospect by Mapel and Hail (1959). The tuff contains ≈1% phenocrysts consisting of 80% sanidine, 10%–15% dipyramidal quartz, and 5%–10% plagioclase. Collected 655 m east of west line and 707 m north of south line, sec. 11, T. 15 S., R. 20 E.; Severe Spring, Idaho, 7.5′ quadrangle; long 114°04.79′W, lat 42°08.06′N.

TC90-40. Sample from the base of a light gray, fine sand-sized, vitric fallout tuff. The tuff includes a basal unit of 1.5 m of parallel laminated fallout tuff and a capping unit of 0.9 m of massive, clayey reworked vitric tuff. Collected 732 m west of east line and 457 m north of south line, sec. 3, T. 15 S., R. 20 E.; Severe Spring, Idaho, 7.5′ quadrangle; long 114°05.80′W, lat 42°08.79′N. (Note: This tuff is duplicated across an east-dipping, high-angle normal fault with 20 m vertical separation. TC90-40 is the third lowest of 10 vitric tuffs exposed in the steep, gullied area where it was sampled. Care must be taken to properly locate the fault zone when resampling this tuff.)

Sections

Violets Hollow Section. N½ sec. 10, S½ sec. 3, W½ sec. 10, and E½ sec. 9, T. 14 S., R. 20 E.

Ibex Hollow Section. S½ sec. 11, S½ sec. 12, N½ sec. 13, and N½ sec. 14, T. 14 S., R. 20 E.

Lower Trapper Creek section. W½ sec. 26, T. 14 S., R. 21 E.

APPENDIX B: CORRELATION OF TUFF BEDS/STATISTICAL DISTANCE

Correlation of Tuff Beds

Approach. Our assessment of the potential correlation between tuffs in different areas is based on both the degree of similarity in the composition of glass shards between samples and on the necessary requirement of homotaxy in a sequence of correlative tuffs. Sarna-Wojcicki and Davis (1991) emphasized the importance of stratigraphic sequence in the correlation of tuff beds, and sequence is particularly important for correlation of a sequence of numerous, often chemically similar tuffs such as those found at Trapper Creek. Our assessment of compositional similarity is based on both the mean composition of glass as measured by X-ray fluorescence (bulk glass) and electron probe microanalysis (≈20 shards) methods, and the pattern of shard-to-shard variation in Ca and Fe revealed by the microprobe analyses. Ca and Fe can show distinct patterns of variation. Our assessment of homotaxy uses a matrix comparing the glass compositions of tuffs in one section with those in another section. Use of such a matrix is quite important. It ensures that all potentially correlative pairs of tuffs are considered and thus minimizes the selection of "false positives" and the deletion of "false negatives" when making a correlation decision.

A numerical assessment in similarity of mean glass composition is done using the statistical distance function, **D**. **D** is simply the Euclidean distance (in standard deviation units) between chemical analyses. Since **D** is a distance function, the smaller the value of **D** between two samples being compared the closer the measured concentration of elements in the two samples. $\mathbf{D} = 0$ indicates an identical concentration of all elements in the samples. With X-ray fluorescence analyses we compared two tuffs using a suite of 11 elements (Ba, Ca, Fe, Mn, Nb, Rb, Sr, Ti, Th, Y, and Zr). These elements generally showed consistent, measurable differences between different tuff beds. With electron probe microanalysis we used a suite of six such elements (Ca, Cl, Fe, Mn, Mg, and Ti); the elements Al and Si were not used in comparison as these elements show little if any variation from tuff to tuff and if used in the distance function (or similarity coefficient) can result in the false impression of a close chemical similarity between two different tuff beds. The elements F, K, and Na are not used in **D** because the concentration of these elements are variably changed during the post-depositional hydration of glass shards.

Assuming that analytical errors are assessed correctly, then, as discussed below for 11 elements, a value of $\mathbf{D} \leq 4.4$ indicates a statistically identical (95% confidence level) glass composition in the two comparison samples, while for 6 elements the corresponding value is $\mathbf{D} \leq 3.5$. These statistical tests are used for mean concentrations (bulk glass for X-ray fluorescence analyses and the mean of ≈20 shards for electron probe analyses). In addition, if two tuffs appear to "match" on the basis of **D**, it is then important to check the pattern of shard-to-shard variation in the concentrations of Fe and Ca. If two samples show a similar shard-to-shard variation in Fe and Ca, then the likelihood that the two samples are from the same tuff layer is further validated.

While a value for $\mathbf{D} \leq 4.4$ (or ≤3.5) is strong evidence for correlation, particularly when there is also a match in shard-to-shard Ca and Fe concentration or when there is some unusual concentration of one or more elements in the tuffs being compared, a larger value for **D** does not rule out possible correlation between two tuffs for one or more reasons. For instance, there may be measurable compositional variation from horizon to horizon in a particular tuff. Such variation, not fully evaluated, is known in some of the Trapper Creek tuffs. Also potentially contributing to higher than expected **D** values are uncertainties in the measurement errors. These errors can vary from run to run on a particular instrument. We used an average estimate of analytical errors that may not always have been appropriate. If the errors are two low for a particular suite of analyses, then calculated values for **D** will be too high. This last problem can be overcome by reanalyzing possibly correlative tuffs during the same instrumental run. The analyses in Table 4, comparing glass composition of Trapper Creek tuffs with potentially correlative tuffs in the Bruneau-Jarbidge area, are such reanalyses.

All of the above techniques and considerations were employed in our comparison of the Trapper Creek tuffs with the sequence of tuffs sampled in the Bruneau-Jarbidge area. The resulting set of stratigraphic, compatible correlations shown in Figure 8 clearly emerged from our analyses of correlation, and we are satisfied that the solid tielines on Figure 8 link correlative tuffs, while the dashed lines link possibly correlative tuffs.

Estimating Analytical Precision. Our estimates of analytical precision (±1 standard deviation) are shown in Tables 3 and 4. Analyses in Table 3 were done over a period of several years and numerous runs on the analytical instruments. The error estimates in Table 3 are average analytical errors for particularly distinctive and widespread SRPVP tuffs that have been identified by us in sections throughout the western United States. The errors in Table 3 (upper half) are average errors for 8 such tuffs, while those in Table 3 (lower half) are average errors for 11 such tuffs. Individual groups of analyses in Table 4 were done during a single run on an instrument. The error estimates in Table 4 are compromise values between the errors in Table 3 and those estimated for a single run of a single sample. Generally, Table 4 errors are smaller than Table 3 errors.

Statistical Distance

The distance function **D** is a Euclidean distance with distance in units of standard deviation. The square of **D** is expressed as follows:

$$\mathbf{D}^2 = \sum_{k=1}^{n} \left[\frac{(x_{k1} - x_{k2})^2}{2\sigma_k^2} \right],$$

where x_{k1} = concentration of element x_k in glass tuff 1, x_{k2} = concentration of element x_k in glass of tuff 2, σ_k = standard deviation for analytical precision of element x_k, and n = number of elements used in the comparison.

$\mathbf{D}^2$ will have a χ^2 distribution with n degrees of freedom, provided the two tuff layers being compared have identical composition and provided analytical errors are estimated precisely and distributed normally.

D (or $\mathbf{D}^2$) provides a theoretically more satisfactory assessment of correlation than the commonly used similarity coefficient, **SC** (Borchardt et al., 1972; Sarna-Wojcicki, 1976; Sarna-Wojcicki et al., 1984; Izett et al., 1987). This is because the similarity coefficient, **SC**, which is defined as

$$\mathbf{SC} = \frac{1}{n} \sum_{k=1} \frac{x_{ki}}{x_{kj}}, \; i, j = 1 \text{ or } 2, \; i \neq j$$

(where x_{ki} is the minimum of the pair x_{k1}, x_{k2}), is a function of both the number of elements included in **SC** and the relative analytical precision (mean/standard deviation) for each of such elements. As relative analytical precision varies from tuff bed to tuff bed because of variation in composition, **SC** has the undesirable characteristic of a variable confidence interval even when a fixed number of elements is used for **SC**. For example, Monte Carlo estimation shows (Perkins, unpubl. data) that the upper tail value for **SC** (with n =

11) at the 95% confidence level is 0.73 when the relative analytical precision of the elements is 0.2 and only rises to >0.93 when the relative analytical precision is >0.02. This variable characteristic of **SC**, even when calculated for a fixed suite of elements, has not been taken into consideration by workers making use of this statistic. An alternative similarity coefficient, termed *RATIONAL*, was proposed by Sarna-Wojcicki et al. (1984). RATIONAL gives higher weighting to those elements with greater analytical precision; however, confidence intervals for RATIONAL are, in the manner of **SC**, dependent on both the number of elements used in the calculation of RATIONAL and the relative analytical precision of these elements. The confidence intervals for **D**, on the other hand, depend only on the number of elements used in a comparison and are independent of relative analytical precision. Hence, the confidence intervals for **D** need not be recalculated for each new tuff bed being compared, something that needs to be done if one wishes to make full use of **SC** or RATIONAL. Further, values for **D** at various confidence levels are easily determined from tables of the chi-square distribution. Such tables are readily available. We prefer to use **D**, but perfectly satisfactory results can be also be obtained using **SC** in the correlation decision, particularly if the variability of the confidence intervals for **SC** is taken into account. While there are some limitations to **SC**, it is worth using in conjunction with **D** because it is much less sensitive to a large difference in concentration of a single element. Such differences can result from errors in data transcription or shortcomings in the purity of a glass separate. If there is a marked disparity between **D** and **SC** for a particular sample, it is worthwhile to reexamine the sample to see what reasons may lie behind the disparity.

For 11 elements a value of $\mathbf{D}^2 \leq 19.7$ (alternatively, $\mathbf{D} \leq 4.4$) indicates that two analyses are statistically identical at the 95% level. For six elements the 95% confidence level range is $\mathbf{D}^2 \leq 12.6$ or, alternatively, $\mathbf{D} \leq 3.5$. For **SC**, Monte Carlo estimates show corresponding ranges of $\mathbf{SC} \geq 0.92$ and $\mathbf{SC} \geq 0.88$ at the 95% confidence level for a Trapper Creek tuff with an average group C glass composition. These values should be kept in mind when examining the tabulated values for **D** and **SC** in Table 4; however, also bear in mind that other factors such as compositional variability from horizon to horizon within a tuff and relative stratigraphic position are also considered in the correlation decision.

REFERENCES CITED

Armstrong, R. L., 1975, The geochronometry of Idaho: Isochron West, v. 14, p. 1–50.

Armstrong, R. L., and Ward, P., 1991, Evolving geographic patterns of Cenozoic magmatism in the North American Cordillera: The temporal and spatial association of magmatism and metamorphic core complexes: Journal of Geophysical Research, v. 96, p. 13201–13224.

Armstrong, R. L., Leeman, W. P., and Malde, H. E., 1975, K-Ar dating, Quaternary and Neogene volcanic rocks of the Snake River Plain, Idaho: American Journal of Science, v. 264, p. 225–251.

Armstrong, R. L., Harakal, J. E., and Neill, W. M., 1980, K-Ar dating of Snake River Plain (Idaho) volcanic rocks—New results: Isochron West, v. 17, p. 5–10.

Axelrod, D. I., 1964, The Miocene Trapper Creek flora of southern Idaho: University of California Publications in the Geological Sciences, v. 51, 148 p.

Bacon, C. R., 1983, Eruptive history of Mount Mazama and Crater Lake caldera, Cascade Range, U.S.A.: Journal of Volcanology and Geothermal Research, v. 18, p. 57–115.

Bacon, C. R., and Duffield, W. A., 1981, Late Cenozoic rhyolites from the Kern Plateau, southern Sierra Nevada, California: American Journal of Science, v. 281, p. 1–34.

Bonnichsen, B., 1981, Stratigraphy and measurements of magnetic polarity for volcanic units in the Bruneau-Jarbidge eruptive center, Owyhee County, Idaho: Idaho Bureau of Mines and Geology Technical Report 81-5, 75 p.

Bonnichsen, B., 1982a, The Bruneau-Jarbidge eruptive center, southwestern Idaho, *in* Bonnichsen, B., and Breckenridge, R. M., eds., Cenozoic geology of Idaho: Idaho Bureau of Mines and Geology Bulletin 26, p. 237–254.

Bonnichsen, B., 1982b, Chemical composition of the Cougar Point Tuff and rhyolite lava flows from the Bruneau-Jarbidge eruptive center, Owyhee County, Idaho: Idaho Bureau of Mines and Geology Open File Report 81-5, 22 p.

Bonnichsen, B., 1982c, Rhyolite lava flows in the Bruneau-Jarbidge eruptive center, southwestern Idaho, *in* Bonnichsen, B., and Breckenridge, R. M., eds., Cenozoic geology of Idaho: Idaho Bureau of Mines and Geology Bulletin 26, p. 237–254.

Bonnichsen, B., and Citron, G. P., 1982, The Cougar Point Tuff, southwestern Idaho and vicinity, *in* Bonnichsen, B., and Breckenridge, R. M., eds., Cenozoic geology of Idaho: Idaho Bureau of Mines and Geology Bulletin 26, p. 255–281.

Bonnichsen, B., and Kauffman, D. F., 1987, Physical features of rhyolite lava flows in the Snake River Plain volcanic province, *in* Fink, J. H., ed., The emplacement of silicic domes and lava flows: Geological Society of America Special Paper 212, p. 119–145.

Borchardt, G. A., Aruscavage, P. J., and Millard, H. T., Jr., 1972, Correlation of the Bishop ash, a Pleistocene marker bed, using instrumental neutron activation analysis: Journal of Sedimentary Petrology, v. 42, p. 303–306.

Campbell, E., 1979, Palynology and paleoecology of the Miocene lignites of the Goose Creek basin, Idaho, Nevada, and Utah [M.S. thesis]: Salt Lake City, University of Utah, 66 p.

Christiansen, R. L., 1984, Yellowstone magmatic evolution: Its bearing on understanding large-volume explosive volcanism, *in* Explosive volcanism: Inception, evolution and hazards: Washington, D.C., National Academy Press, Studies in Geophysics, p. 84–95.

Coats, R. R., 1964, Geology of the Jarbidge quadrangle, Nevada-Idaho: U.S. Geological Survey Bulletin 1141-M, 24 p.

Coney, P. J., 1978, Mesozoic–Cenozoic Cordilleran plate tectonics: Geological Society of America Memoir 152, p. 33–50.

Coney, P. J., and Harms, T., 1984, Cordilleran metamorphic core complexes: Cenozoic extensional relics of Mesozoic compression: Geology, v. 12, p. 550–554.

Dalrymple, G. B., and Duffield, W. A., 1988, High precision $^{40}Ar/^{39}Ar$ dating of Oligocene rhyolites from the Mogollon-Datil volcanic field using a continuous laser system: Geophysical Research Letters, v. 15, p. 463–466.

Duffield, W. A., and Ruiz, J., 1992, Composition gradients in large reservoirs of silicic magma as evidenced by ignimbrites versus Taylor Creek Rhyolite lava domes: Contributions to Petrology, v. 110, 192–210.

Ekren, E. B., McIntyre, D. H., and Bennett, E. H., 1984, High-temperature, large-volume, lavalike ash-flow tuffs without calderas in southwestern Idaho: U.S. Geological Survey Professional Paper 1272, 76 p.

Elison, M. W., Speed, R. C., and Kistler, R. W., 1990, Geologic and isotopic constraints on the crustal structure of the northern Great Basin: Geological Society of America Bulletin, v. 102, p. 1077–1092.

Farmer, G. L., and DePaolo, D. J., 1983, Origin of Mesozoic and Tertiary granite in the western United States and implications for pre-Mesozoic crustal structure 1. Nd and Sr isotopic studies in the geocline of the northern Great Basin: Journal of Geophysical Research, v. 88, p. 3379–3401.

Hackett, W. R., and Morgan, L. A., 1988, Explosive basaltic and rhyolitic volcanism of the eastern Snake River Plain, Idaho, *in* Link, P. K., and Hackett, W. R., eds., Guidebook to the geology of central and southern Idaho: Idaho Geological Survey Bulletin 27, p. 283–301.

Hackett, W. R., Moye, F. J., and Bonnichsen, B., 1989, Silicic volcanics around the Cassia Mountains, *in* Chapin, C. E., and Zidek, J., eds., Field excursions to volcanic terranes in the western United States, Vol. II; Cascades and intermountain West: New Mexico Bureau of Mines and Mineral Resources Memoir 47, p. 135–137.

Hildebrand, R. T., and Newman, K. R., 1985, Miocene sedimentation in the Goose Creek basin, south-central Idaho, northeastern Nevada and northwestern Utah, *in* Flores, R. M., et al., eds., Cenozoic paleogeography of the western U.S.: Rocky Mountain Section, Society of Economic Paleontologists and Mineralogists, p. 55–70.

Hildreth, W., 1981, Gradients in silicic magma chambers: Implications for lithospheric magmatism: Journal of Geophysical Research, v. 86, p. 10153–10192.

Hildreth, W., Halliday, A. N., Christiansen, R. L., 1991, Isotopic and chemical evidence concerning the genesis and contamination of basaltic and rhyolitic magma beneath the Yellowstone Plateau volcanic field: Journal of Petrology, v. 32, p. 63–138.

Honjo, N., 1990, Geology and stratigraphy of the Mount Bennett Hills, and the origin of west-central Snake River Plain rhyolites [Ph.D. thesis]: Houston, Texas, Rice University, 259 p.

Honjo, N., Bonnichsen, B., Leeman, W. P., and Stormer, J. C., Jr., 1992, Mineralogy and geothermometry of high-temperature rhyolites from the central and western Snake River Plain: Bulletin of Volcanology, v. 54, p. 220–237.

Izett, G. A., 1981, Volcanic ash beds: Recorders of upper Cenozoic silicic pyroclastic volcanism in the western United States: Journal of Geophysical Research, v. 86, p. 10200–10222.

Izett, G. A., and Wilcox, R. A., 1982, Map showing localities and inferred distribution of the Huckleberry Ridge, Mesa Falls, and Lava Creek ash beds (Pearlette family ash beds) of Pliocene and Pleistocene age in the western United States and Canada: U.S. Geological Survey Miscellaneous Investigations Map I-1325, scale 1:4 000 000.

Izett, G. A., Obradovich, J. D., and Mehnert, H. H., 1988, The Bishop Ash bed (middle Pleistocene) and some older (Pliocene and Pleistocene) chemically and mineralogically similar ash beds in California, Nevada, and Utah: U.S. Geological Survey Bulletin 1675, 37 p.

Kaufman, L., and Rousseeuw, P. J., 1990, Finding groups in data: An introduction to cluster analysis: New York, Wiley, 342 p.

Lanphere, M. A., Dalrymple, G. B., Fleck, R. J., and Pringle, M. S., 1990, Intercalibration of mineral standards for K-Ar and $^{40}Ar/^{39}Ar$ age measurements [abs.]: EOS (American Geophysical Union Transactions), v. 71, no. 43, p. 1658.

Leeman, W. P., 1982a, Development of the Snake River Plain Yellowstone Plateau province, Idaho and Wyoming: An overview and petrologic model, *in* Bonnichsen, B., and Breckenridge, R. M., eds., Cenozoic geology of Idaho: Idaho Bureau of Mines and Geology Bulletin 26, p. 155–157.

Leeman, W. P., 1982b, Rhyolites of the Snake River Plain–Yellowstone Plateau province, Idaho and Wyoming: A summary of petrogenetic models, *in* Bonnichsen, B., and Breckenridge, R. M., eds., Cenozoic geology of Idaho: Idaho Bureau of Mines and Geology Bulletin 26, p. 203–212.

Leeman, W. P., Oldow, J. S., and Hart, W. K., 1992, Lithosphere-scale thrusting in the western U.S. Cordillera as constrained by Sr and Nd isotopic transitions in Neogene volcanic rocks: Geology, v. 20, p. 63–66.

Lerbekmo, J. F., Westgate, J. A., Smith, D. G. W., and Benton, G. H., 1975, New data on the character and history of the White River volcanic eruption, Alaska, *in* Cresswell, M. M., and Suggate, R. P., eds., Quaternary studies: Royal Society of New Zealand, p. 203–209.

Luedke, R. G., and Smith, R. L., 1981, Map showing distribution, composition, and age of late Cenozoic volcanic centers in California and Nevada: U.S. Geological Survey Miscellaneous Investigations Map I-1091-C, 2 sheets, scale 1:1 000 000.

Luedke, R. G., and Smith, R. L., 1982, Map showing distribution, composition, and age of late Cenozoic volcanic centers in Oregon and Washington: U.S. Geological Survey Miscellaneous Investigations Map I-1091-D, 1 sheet, scale 1:1 000 000.

Luedke, R. G., and Smith, R. L., 1983, Map showing distribution, composition, and age of late Cenozoic volcanic centers in Idaho, western Montana, west-central South Dakota, and northwestern Wyoming: U.S. Geological Survey Miscellaneous Investigations Map I-1091-E, 2 sheets, scale 1:1 000 000.

Malde, H. E., 1986, Quaternary geology and structural history of the Snake River Plain, Idaho and Oregon, *in* Morrison, R. B., ed., Quaternary nonglacial geology: Conterminous U.S.: Boulder, Colorado, Geological Society of America, Geology of North America, v. K-2, p. 251–281.

Malde, H. E., and Powers, H. A., 1962, Upper Cenozoic stratigraphy of western Snake River Plain, Idaho: Geological Society of America Bulletin, v. 73, p. 1197–1220.

Manley, C. R., 1992, A low temperature rhyolite lava flow mimicking a high-temperature rheomorphic ignimbrite: The Badlands Lava, Owyhee Plateau, SW Idaho [abs.]: EOS (American Geophysical Union Transactions), v. 73, p. 636.

Mapel, W. J., and Hail, W. J., 1959, Tertiary geology of the Goose Creek District, Cassia County, Idaho, Box Elder County, Utah, and Elko County, Nevada: U.S. Geological Survey Bulletin 1055-H, p. H217–H254.

Morgan, L. A., 1992, Stratigraphic relations and paleomagnetic and geochemical correlations of ignimbrites of the Heise volcanic field, eastern Snake River Plain, eastern Idaho and western Wyoming, *in* Link, P. K., Kuntz, M. A., and Platt, L. B., eds., Regional geology of eastern and western Wyoming: Geological Society of America Memoir 179, p. 215–225.

Morgan, L. A., Doherty, D. J., and Leeman, W. P., 1984, Ignimbrites of the eastern Snake River Plain: Evidence for major caldera-forming eruptions: Journal of Geophysical Research, v. 89, p. 8665–8678.

Morgan, P., 1972, Deep mantle convection plumes and plate motions: American Association of Petroleum Geologists Bulletin, v. 56, p. 203–213.

Mytton, J. W., Williams, P. L., and Morgan, W. A., 1990, Geologic map of the Stricker 4 quadrangle, Cassia, Twin Falls, and Jerome Counties, Idaho: U.S. Geological Survey Miscellaneous Investigations Series Map I-2052, scale 1:48 000.

Nash, W. P., 1992, Analysis of oxygen with the electron microprobe: Application to hydrous glass and minerals: American Mineralogist, v. 77, p. 453–457.

Nash, W. P., Perkins, M. E., and Brown, F. H., 1993, Frequency and composition of explosive eruptions from the Yellowstone hotspot from 14 to 0 Ma [abs.]: EOS (American Geophysical Union Transactions), v. 74, p. 593.

Ninkovich, D., Sparks, R. S. J., and Ledbetter, M. T., 1978, The exceptional magnitude and intensity of the Toba eruption,

Sumatra: An example of the use of deep-sea tephra layers as a geological tool: Bulletin of Volcanology, v. 41, p. 286–298.
Perkins, M. E., Brown, F. H., and Nash, W. P., 1993, Miocene tephrochronology in the northern Basin and Range: Geological Society of America Abstracts with Programs, v. 25, no. 5, p. 133.
Perkins, M. E., Diffendahl, R. F., and Voorhies, M. R., 1995, Tephrochronology of the Ash Hollow Formation (Ogallala Group)—Northern Great Plains: Geological Society of America Abstracts with Programs, v. 27, no. 3, p. 79.
Pierce, K. L., and Morgan, L. A., 1992, The track of the Yellowstone hot spot: Volcanism, faulting, and uplift, *in* Link, P. K., Kuntz, M. A., and Platt, L. B., eds., Regional geology of eastern and western Wyoming: Geological Society of America Memoir 179, p. 1–53.
Rodgers, D. W., Hackett, W. R., and Ore, H. T., 1990, Extension of the Yellowstone Plateau, eastern Snake River Plain, and Owyhee Plateau: Geology, v. 18, p. 1138–1141.
Rodgers, D. W., Ore, H. T., Bobo, R., Henderson, E. P., and Huerta, A. D., 1991, Drainage reversal in three Basin and Range grabens, southeastern Idaho: Evidence for Miocene passage of the Yellowstone hot spot: Geological Society of America Abstracts with Programs, v. 23, no. 4, p. 88.
Rose, W. I., and Chesner, C. A., 1987, Dispersal of ash in the great Toba eruption, 75 ka: Geology, v. 15, p. 913–917.
Rose, W. I., Grant, N. K., and Easter, J., 1979, Geochemistry of the Los Chocoyos Ash, Quezaltenango Valley, Guatemala, *in* Chapin, C. E., and Elston, W. E., eds., Ash-flow tuffs: Geological Society of America Special Paper 180, p. 87–99.
Rytuba, J. J., and McKee, E. H., 1984, Peralkaline ash flow tuffs and calderas of the McDermitt volcanic field, southeast Oregon and north central Nevada: Journal of Geophysical Research, v. 89, p. 8616–8628.
Saltzer, S. D., and Hodges, K. V., 1988, The Middle Mountain shear zone, southern Idaho: Kinematic analysis of an early Tertiary high-temperature detachment: Geological Society of America Bulletin, v. 100, p. 96–103.
Sampson, S. D., and Alexander, E. C., 1987, Calibration of the interlaboratory $^{40}Ar/^{39}Ar$ dating standard, MMhb-1: Chemical Geology, v. 66, p. 27–34.
Sarna-Wojcicki, A. M., 1976, Correlation of late Cenozoic tuffs in the central Coast Ranges of California by means of trace- and minor-element chemistry: U.S. Geological Survey Professional paper 972, 30 p.
Sarna-Wojcicki, A. M., and Davis, J. O., 1991, Quaternary tephrochronology, *in* Morrison, R. B., ed., Quaternary nonglacial geology: Conterminous U.S.: Boulder, Colorado, Geological Society of America, Geology of North America, v. K-2, p. 93–116.
Sarna-Wojcicki, A. M., and nine others, 1984, Chemical analyses, correlations, and ages of Pliocene and Pleistocene ash layers of east-central and southern California, U.S. Geological Survey Professional Paper 1293, 41 p.
Schlinger, C. M., Griscom, D., Papaefthymiou, G., and Veblen, D. R., 1988, The nature of magnetic single-domains in volcanic glasses of the KBS tuff: Journal of Geophysical Research, v. 93, p. 9137–9156.
Smith, R. B., and Braille, L. W., 1993, Topographic signature, space-time evolution, and physical properties of the Yellowstone–Snake River Plain volcanic system: The Yellowstone hotspot, *in* Snoke, A. W., Steidtman, J. R., and Roberts, S. M., eds., Geology of Wyoming: Geological Survey of Wyoming Memoir 5, p. 695–754.
Smith, R. P., and Nash, W. P., 1976, Chemical correlation of volcanic ash deposits in the Salt Lake Group, Utah, Idaho and Nevada: Journal of Sedimentary Petrology, v. 46, p. 930–939.
Steiger, R. H., and Jager, E., 1977, Subcommission on geochronology: Convention on the use of decay constants in geo- and cosmochronology: Earth and Planetary Science Letters, v. 36, p. 362.
Warshaw, C. M., and Smith, R. L., 1988, Pyroxenes and fayalites in the Bandelier Tuff, New Mexico: Temperatures and comparison with other rhyolites: American Mineralogist, v. 73, p. 1025–1037.
Watson, E. B., and Harrison, T. M., 1983, Zircon saturation revisited: Temperature and composition effects in a variety of crustal magma types: Earth and Planetary Science Letters, v. 64, p. 295–304.
Westgate, J. A., and Naeser, N. D., 1985, Tephrochronology and fission-track dating, *in* Nathaniel Rutter, N. W., ed., Dating methods of Pleistocene deposits and their problems: Geoscience Canada, Reprint Series 2, p. 31–38.
Williams, P. L., Mytton, J. W., and Covington, H. R., 1990, Geologic map of the Stricker 1 quadrangle, Cassia, Twin Falls, and Jerome Counties, Idaho: U.S. Geological Survey Miscellaneous Investigations Map I-2078, scale 1:48 000.

MANUSCRIPT RECEIVED BY THE SOCIETY NOVEMBER 9, 1994
REVISED MANUSCRIPT RECEIVED MARCH 22, 1995
MANUSCRIPT ACCEPTED MARCH 31, 1995

Printed in U.S.A.